RUHR UNIVERSITÄT BOCHUM

RUB

Doubly Heavy Tetraquarks from Lattice QCD Scattering Data: An EFT Analysis

Vadim Baru

Institut für Theoretische Physik II

Ruhr-Universität Bochum Germany

Beijing, September 21, 2026

Workshop on Few-Body Problems in Nuclear and Hadron Physics

Largely based on PRD 113, 114041 (2026), PRD 109, L071506 (2024)

see also PLB 860, 139188 (2025), PRL 131, 131903 (2023), PRD 111, 034509 (2025)

in collaboration with: M. Abolnikov, E. Epelbaum, A. Filin, A. Gasparyan, L. Meng from Bochum and

X. Dong, M. Du, F.-K. Guo, C. Hanhart, A. Nefediev, J. Nieves, E. Ortiz-Pacheco, M. Padmanath, S. Prelovsek and Q. Wang

Doubly Heavy Exotic States

–Predicted since 1980's: Ader, Lipkin, Karliner, Eichten, Manohar, Wise, … see reviews Francis Prog. Part. Nucl. Phys. (2025) Bicudo et al., Phys. Rept. (2023)

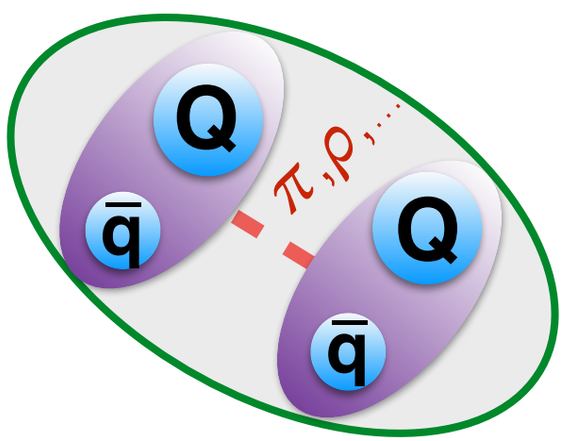
- cc-quark T_{cc} A shallow state near DD* thr LHCb Exp many Lattice data $cc\bar{q}\bar{q}$
- bc-quark T_{bc} Some controversial results Only Lattice data $bc\bar{q}\bar{q}$

(Shallow) bound states from FV spectra Alexandrou et al 2024; Padmanath et al 2024

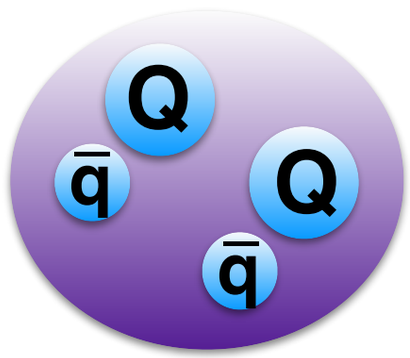
Deeply virtual states from Born-Oppenheimer Hoffmann et al. 2025

- bb-quark T_{bb} Deeply bound states Only Lattice data $bb\bar{q}\bar{q}$

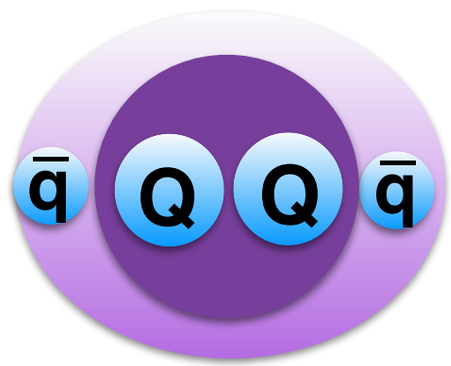
Francis Prog. Part. Nucl. Phys. (2025)



molecule



tetraquark



hadroquarkonium . . .

Size: $\sim 1/\sqrt{2\mu E_B} >> 1\text{fm}$ $\sim 1/\Lambda_{\text{QCD}} \sim 1\text{fm}$

T_{cc} from experiment and lattice

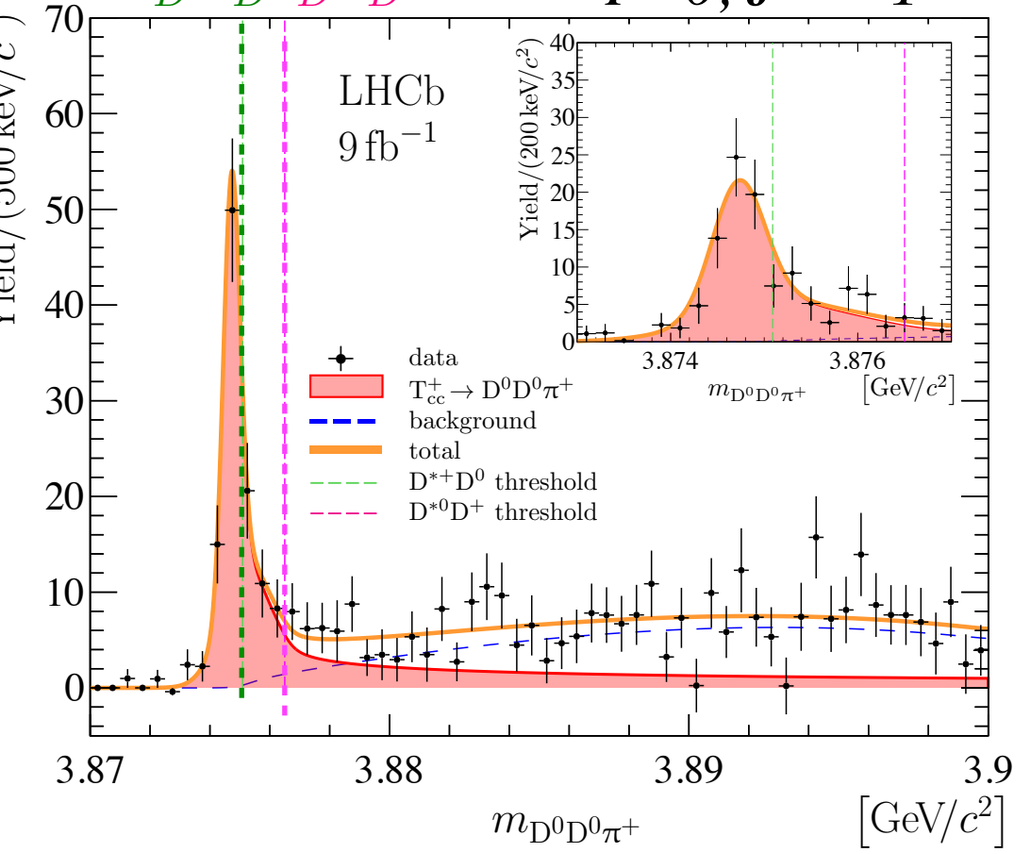
LHCb Nature Physics, Nature Comm.(2022)

$$\delta m_{\rm pole} = -360 \pm 40^{+4}_{-0}\ {\rm keV}$$

$$\Gamma_{\rm pole} = 48 \pm 2^{+0}_{-14}\ {\rm keV}$$

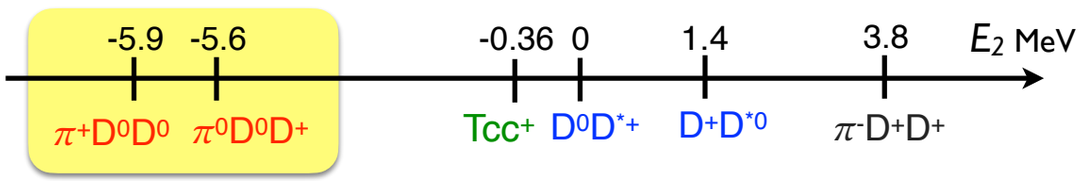
$ccq\bar{q}$

$D^{*+}D^0$ $D^{*0}D^+$ $I=0, J^P = 1^+$



— Width: almost entirely from the only strong decay

$$T_{cc}^+ \to D^0 D^{*+} \to D^0 D^0 \pi^+ / D^0 D^+ \pi^0$$



our LO EFT with full DDπ: Du, VB, et al. *PRD* 105, 014024 (2022)

$$\delta m_{\rm pole} = -356^{+39}_{-38}\ {\rm keV}$$

$$\Gamma_{\rm pole} = 56 \pm 2\ {\rm keV}$$

HAL QCD , *PRL* 131 161901 (2023)

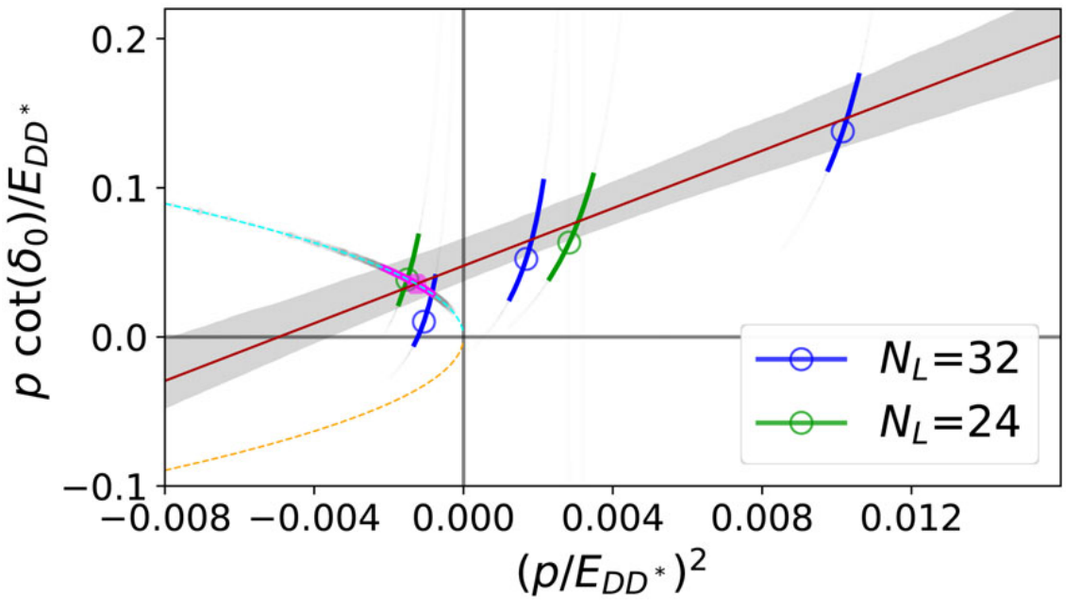
Padmanath and Prelovsek, PRL 129, 032002 (2022)

HadSpec: *PRD* 111, 034511 (2025)

CLQCD: PLB 833 2022

HAL QCD and FV spectra (+ Lüscher + ERE):
neglecting long-range effect

m_π = 146 MeV, 280 MeV, 350 MeV, 391 MeV



T_{cc} is a DD* virtual state

T_{cc}' is a D*D* resonance HadSpec

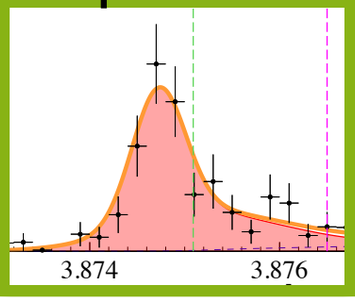
see also more recent calculations

Collins et al PRD 109, 094509 (2024)
Prelovsek et al PRD 112, 014507 (2025)

Alharazin et al arXiv:2602.17204v1 (2026)

χEFT in the infinite and finite volumes

Experiment



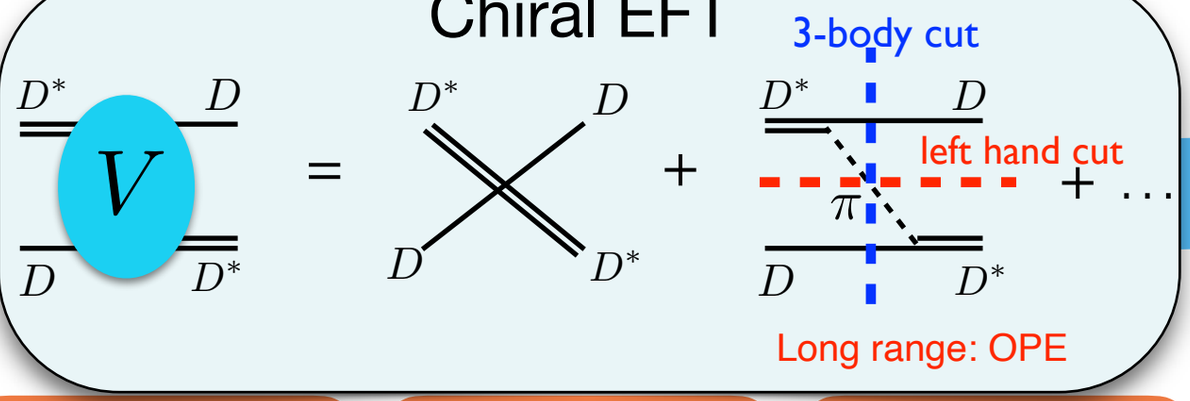
Finite volume



✓ three-body cuts

✓ range corrections

Chiral EFT



✓ left-hand cuts

✓ $\exp(-\mu L)$ corrections

✓ partial wave mixing

- ERE parameters
- Pole positions
- Spin partners
- Chiral Extrapolations

Understanding near-threshold states calls for:

- Impact of long range interactions with their left and right hand cuts on the amplitudes
- Exotic properties from experiment and lattice within the same framework
- Light-quark mass dependence

χEFT as an alternative to Lüscher: Meng, VB, Filin, Epelbaum, Gasparyan *PRD letter* 109, L071506 (2024)

— the Lüscher method is invalid at least below the lhc
Green et al (2021), Raposo and Hansen (2023), Dawid et al. (2023), Meng, VB et al (2023), …

— the ERE convergence is limited by the lhc
Du, VB, et al. *PRL* 131 (2023)

⇒ Both solved ✓

Two examples of recent lattice data analyses

- ChEFT analysis of DD* FV spectra at $m_\pi = 280$ MeV

Isoscalar case: Attraction leading to T_{cc}

PHYSICAL REVIEW D **109,** L071506 (2024)

Letter

Solving the left-hand cut problem in lattice QCD: $T_{cc}(3875)^+$ from finite volume energy levels

Lu Meng, Vadim Baru, Evgeny Epelbaum, Arseniy A. Filin, and Ashot M. Gasparyan
Institut für Theoretische Physik II, Ruhr-Universität Bochum, D-44780 Bochum, Germany

(Received 11 December 2023; accepted 3 April 2024; published 30 April 2024)

We discuss a novel effective-field-theory-based approach for extracting two-body scattering information from finite volume energies, serving as an alternative to Lüscher's method. By explicitly incorporating one-pion exchange, we overcome the challenging left-hand cut problem in Lüscher's method and can handle finite volume energy levels both below and above the left-hand cut. Applied to the lattice data for DD^* scattering at a pion mass of 280 MeV, as an illustrative example, our results reveal the significant impact of the one-pion exchange on P-wave and S-wave phase shifts. The pole position of the $T_{cc}(3875)^+$ state, extracted from the finite-volume energy levels at this pion mass while taking into account left-hand cut effects, range corrections and partial-wave mixing, is consistent with a near-threshold resonance. This study demonstrates, for the first time, that two-body scattering information can be reliably extracted from lattice spectra including the left-hand cut.

DOI: 10.1103/PhysRevD.109.L071506

Phys. Lett. B 860 (2025) 139188

Contents lists available at ScienceDirect

Physics Letters B

journal homepage: www.elsevier.com/locate/physletb

Letter

Internal structure of the $T_{cc}(3875)^+$ from its light-quark mass dependence

Michael Abolnikov [a], Vadim Baru [a,b,*], Evgeny Epelbaum [a], Arseniy A. Filin [a], Christoph Hanhart [b], Lu Meng [a]

[a] Institut für Theoretische Physik II, Ruhr-Universität Bochum, D-44780 Bochum, Germany
[b] Institute for Advanced Simulation (IAS-4), Forschungszentrum Jülich, D-52425 Jülich, Germany

ARTICLE INFO

Editor: B. Grinstein

ABSTRACT

We employ a chiral effective field theory-based approach to connect DD^* scattering observables at the physical and variable pion masses accessible in lattice QCD simulations. We incorporate all relevant scales associated with three-body $DD\pi$ dynamics and the left-hand cut induced by the one-pion exchange for pion masses higher than the physical one, as required by analyticity and unitarity. By adjusting the contact interactions to match experimental data at the physical pion mass and lattice finite-volume energy levels at $m_\pi = 280$ MeV, we predict the trajectory of the T_{cc} pole as a function of the pion mass, finding it consistent with the hadronic-molecule scenario. In particular, we find that the explicit treatment of the one-pion exchange has a pronounced effect on the pole trajectory for $m_\pi \gtrsim 230$ MeV by pushing it into the complex energy plane.

Isovector case: Repulsion

PHYSICAL REVIEW D **111,** 034509 (2025)

Doubly charm tetraquark channel with isospin 1 from lattice QCD

Lu Meng [1,*] Emmanuel Ortiz-Pacheco [2,3,†] Vadim Baru [1] Evgeny Epelbaum [1] M. Padmanath [4,5,‡] and Sasa Prelovsek [2,6,§]

[1] *Institut für Theoretische Physik II, Ruhr-Universität Bochum, D-44780 Bochum, Germany*
[2] *Jozef Stefan Institute, Jamova 39, 1000 Ljubljana, Slovenia*
[3] *Department of Physics and Astronomy, Michigan State University, East Lansing, 48824, Michigan, USA*
[4] *The Institute of Mathematical Sciences, CIT Campus, Chennai, 600113, India*
[5] *Homi Bhabha National Institute, Training School Complex, Anushaktinagar, Mumbai 400094, India*
[6] *Faculty of Mathematics and Physics, University of Ljubljana, 1000 Ljubljana, Slovenia*

(Received 20 November 2024; accepted 23 January 2025; published 19 February 2025)

Experimentally, the doubly charm tetraquark channel $cc\bar{q}\bar{q}$ with $q = u, d$ features an exotic hadron, T_{cc}, with isospin $I = 0$ near the DD^* threshold, while no peak was observed for $I = 1$. We present a lattice QCD study of this channel with $I = 1$, $J^P = 1^+$, and $m_\pi \simeq 280$ MeV. Finite-volume energies calculated across five charm quark masses consistently feature a positive energy shift with respect to noninteracting energies, indicating repulsive interaction at energies near the threshold. These energies are used to compute the DD^* scattering amplitude using both the standard Lüscher method and the recently proposed effective field theory-based approach in the plane wave basis, which incorporates the long-range interactions and the left-hand cut. Both analyses render a small negative scattering length and a scattering amplitude that does not feature any poles in the energy region near the DD^* threshold, in line with the LHCb results. We identify that the Wick contraction, resembling t-channel isovector-vector meson exchanges between D and D^*, plays a key role in distinguishing between the $I = 0$ and $I = 1$ channels, leading to repulsion in the $I = 1$ and attraction in the $I = 0$ channel.

DOI: 10.1103/PhysRevD.111.034509

- Coupled-channel ChEFT analysis of $D^{(*)}B^{(*)}$ scattering on lattice: T_{bc}

PHYSICAL REVIEW D **113,** 114041 (2026)

Shallow T_{bc} states from an EFT analysis of $B^{(*)}\bar{D}^{(*)}$ scattering on the lattice

Michael Abolnikov,[1] Lu Meng,[1,2] Vadim Baru,[1] Evgeny Epelbaum,[1] Arseniy A. Filin,[1] and Ashot M. Gasparyan[1]

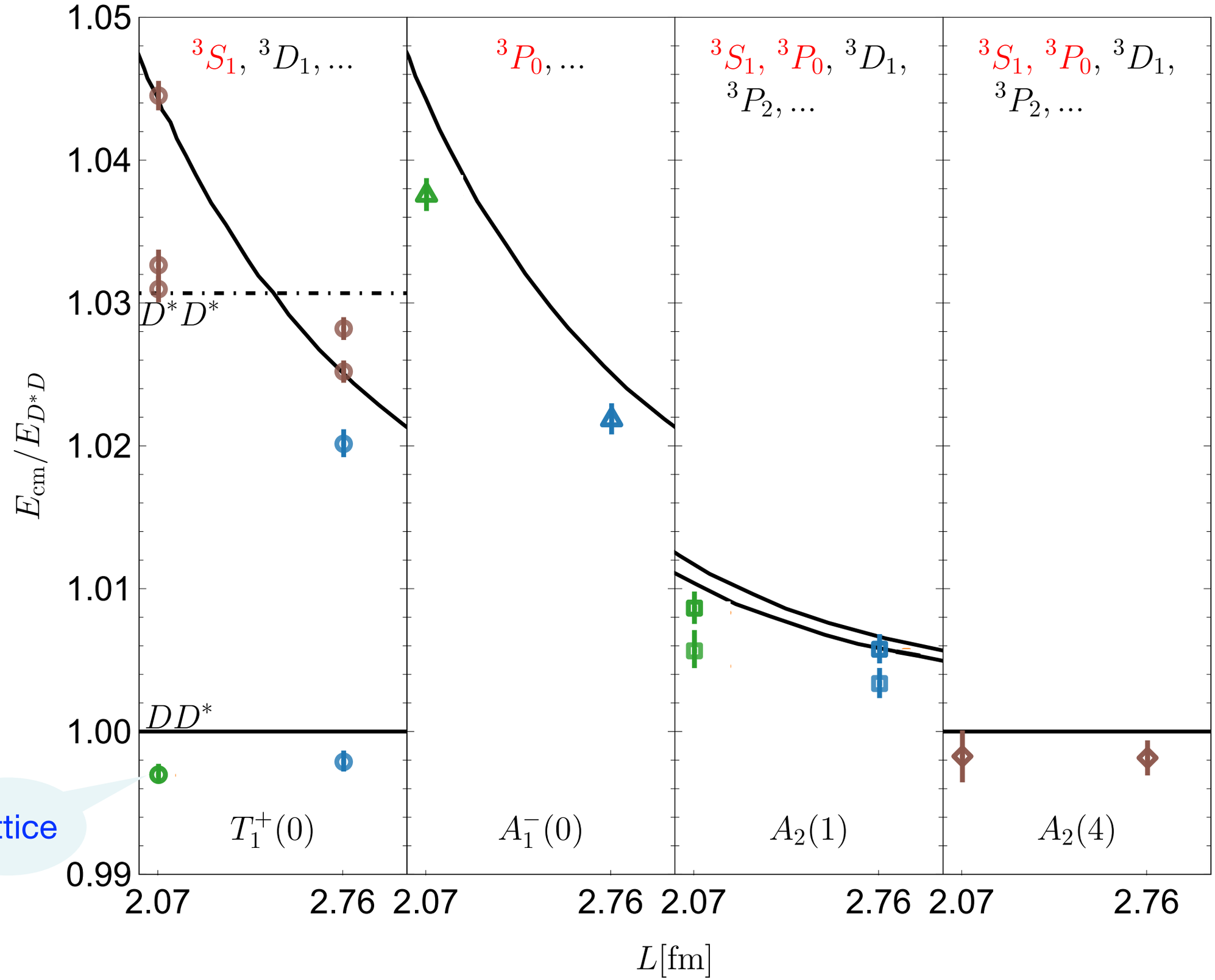
[1] *Institut für Theoretische Physik II, Ruhr-Universität Bochum, D-44780 Bochum, Germany*
[2] *School of Physics, Southeast University, Nanjing 211189, China*

(Received 9 February 2026; accepted 7 May 2026; published 22 June 2026)

We present an effective field theory (EFT) framework for coupled-channel $B^{(*)}\bar{D}^{(*)}$ scattering, applying it to recent lattice QCD results by Alexandrou *et al.* [Phys. Rev. Lett. **132**, 151902 (2024)]. Two complementary EFT approaches are developed: (1) a low-energy theory near the $B\bar{D}$ ($J = 0$) and $B^*\bar{D}$ ($J = 1$) thresholds, where coupled-channel effects are integrated out; (2) coupled-channel formulation, where all relevant momentum scales are treated as soft, incorporating contact interactions and one-pion exchange (OPE). Importantly, OPE contributes to the lowest channels only through off-diagonal transitions, thus resulting in the appearance of the left-hand cut from two-pion exchange. The two approaches yield mutually consistent results, supporting the existence of shallow bound states in both channels, in agreement with the lattice findings. The finite-volume spectra and extracted pole positions show a near-degeneracy in $J = 0$ and $J = 1$ channels, consistent with heavy-quark spin symmetry (HQSS). Using HQSS, we predict additional shallow bound states near the $B\bar{D}^*$ and $B^*\bar{D}^*$ thresholds, which are accessible to future lattice simulations. The effect of OPE on the finite volume spectra is found to be small, with only moderate impact on HQSS partners.

I=0 DD* FV E-Levels at $m_\pi = 280$ MeV

Meng, VB, Filin, Epelbaum and Gasparyan *PRD letter* 109, L071506 (2024)



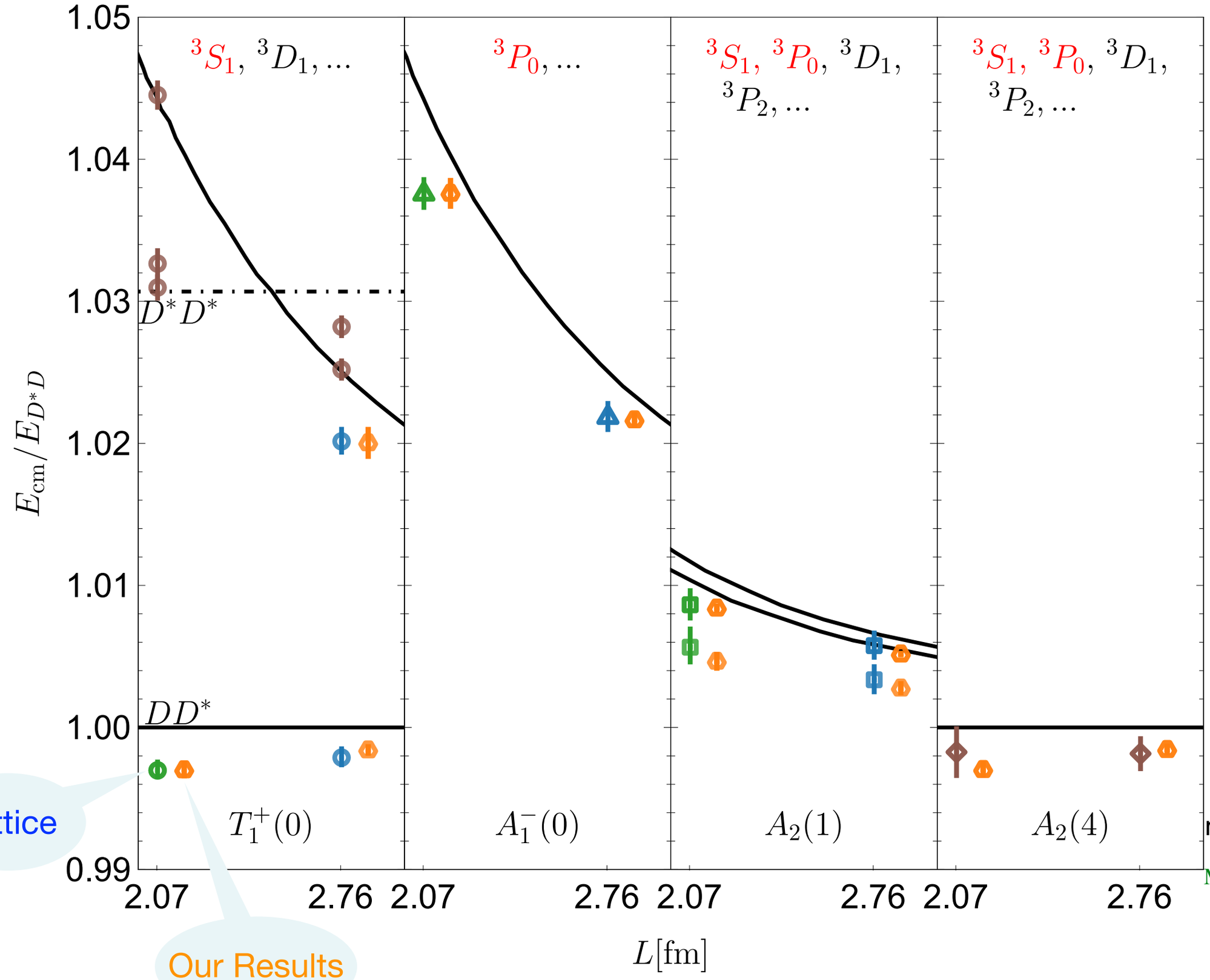
Lattice

Lattice

Padmanath and Prelovsek, PRL 129, 032002 (2022)

I=0 DD* FV E-Levels at $m_\pi = 280$ MeV

Meng, VB, Filin, Epelbaum and Gasparyan *PRD letter* 109, L071506 (2024)



Lattice

Padmanath and Prelovsek, PRL 129, 032002 (2022)

- Our Results at NLO χEFT

3 contact terms:

2 in $^3S_1$

1 in $^3P_0$

—E_{FV} as eigenvalues

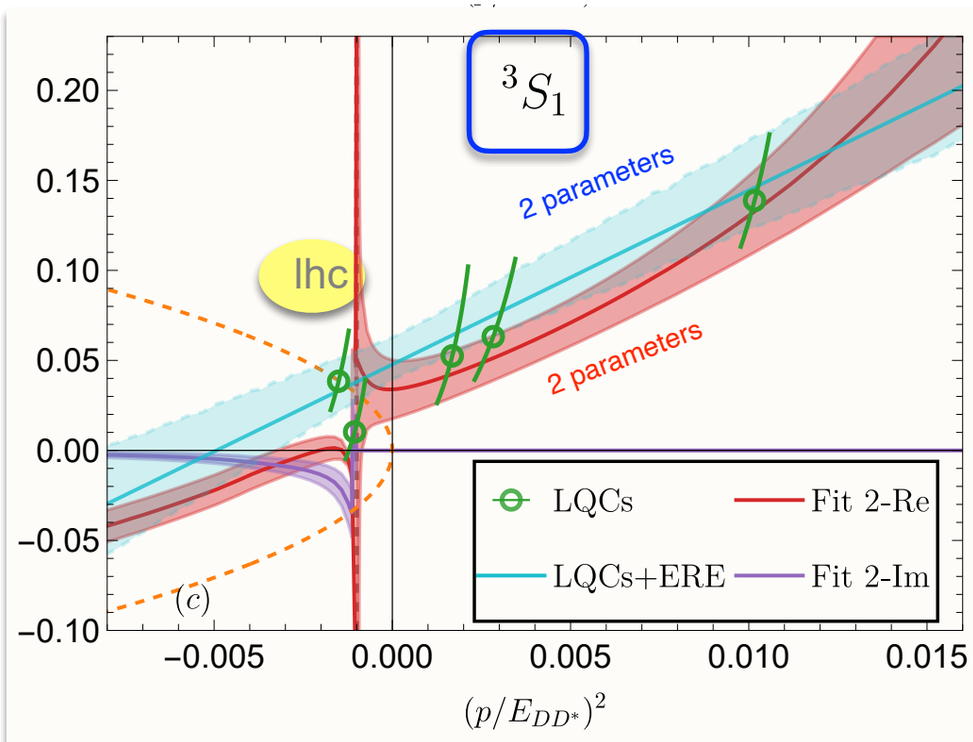
$$\det\left[\mathbb{G}^{-1}(E) - \mathbb{V}(E)\right] = 0$$

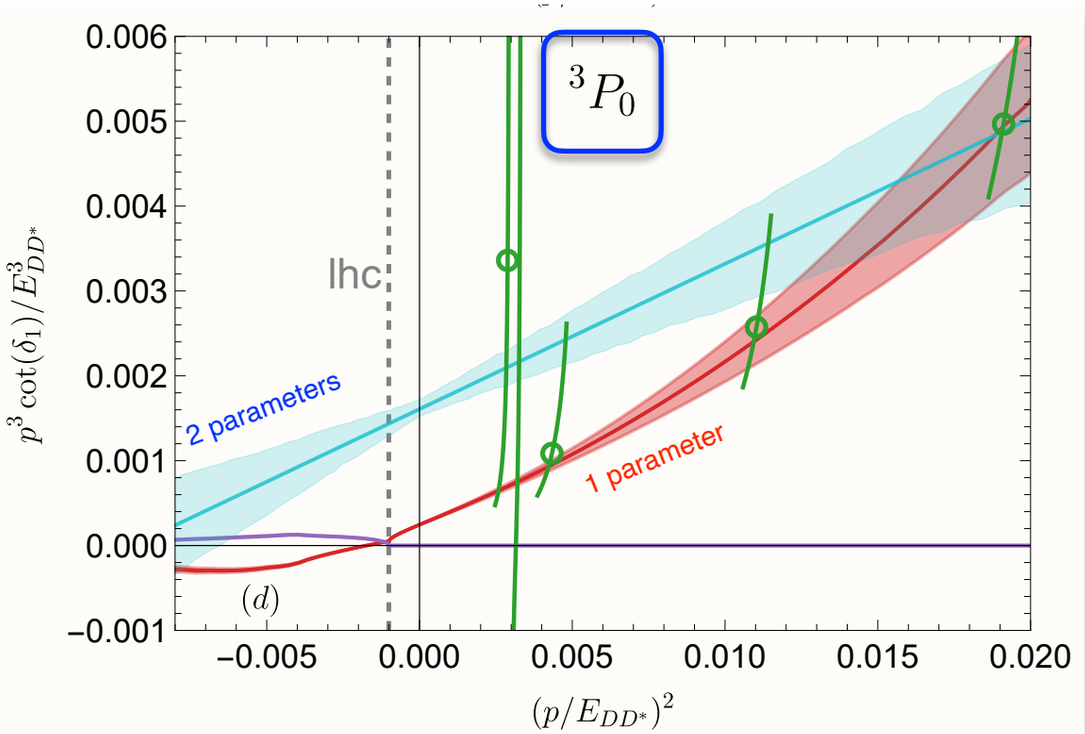
—Plane-wave basis:

no PW truncation in OPE

Meng and Epelbaum JHEP (2021

Predictions: Inf. volume phase shifts for I=0 DD* scatt.





Lüscher+ERE
Padmanath and Prelovsek

our 1σ band
With OPE

- systematic errors also included (small)

- $^3S_1$ near threshold strongly affected by OPE
- $^3P_0$ shape controlled by OPE

	$a_{^3S_1}$ [fm]	$r_{^3S_1}$ [fm]	$\delta m_{T_{cc}}$ [MeV]	$a_{^3P_0}$ [fm^3]	$r_{^3P_0}$ [fm^{-1}]	χ^2/dof	# of param's
LQCs+ERE fit [23]	1.04 ± 0.29	$0.96^{+0.18}_{-0.20}$	$-9.9^{+3.6}_{-7.2}$	$0.076^{+0.008}_{-0.009}$	6.9 ± 2.1	3.7/5	4
Fit 1: cont.	1.09 ± 0.35	0.75 ± 0.14	-10.6 ± 4.4	0.028 ± 0.004	-4.3 ± 0.05	5.52/6	3
Fit 2: cont.+OPE	1.46 ± 0.57	0.096 ± 0.53	$-6.6(\pm 1.5) - i4.0(\pm 3.7)$	0.497 ± 0.007	5.63 ± 0.19	2.95/6	3

[23] Padmanath and Prelovsek, PRL 129, 032002 (2022)

Meng, VB, Filin, Epelbaum and Gasparyan *PRD letter* 109, L071506 (2024)

T_{cc} at $m\pi = 280$ MeV is a resonance state with 85% probability

⇒ Significant influence of the long-range physics

Chiral extrapolations of the Tcc pole

M. Abolnikov, VB, E. Epelbaum, A. Filin, C. Hanhart and L. Meng PLB 860, 139188 (2025)

- Employ knowledge of the NLO potential from our two analyses at

$$m_\pi = m_\pi^{\rm ph}$$
$$m_\pi = 280 \text{ MeV}$$

Du et al. *PRD* 105, 014024 (2022); Meng et al. 109, L071506 (2024)

$$V_{\rm cont}^{(0)+(2)}[^3S_1] = \underbrace{C_{^3S_1}^{(0)}}_{m_\pi = m_\pi^{\rm ph}} + \underbrace{C_{^3S_1}^{(2)}(p^2+p'^2) + D_{^3S_1}^{(2)}(\xi^2-1)}_{m_\pi = 280 \text{ MeV}}$$

$$\xi = \frac{m_\pi}{m_\pi^{\rm ph}}$$

- Take care of m_π dependence of $g_{D^*D\pi}$, $m_{D(*)}$ and f_π in $V_{\rm OPE}$

Becirevic and Sanfilippo PLB 721, 94 (2013)
VB et al., PLB 726, 537 (2013)

Meng et al, *PRD letter* 109, L071506 (2024)

- Calculate scattering amplitude for any m_π including both three-body and left-hand cuts

Disclaimer: Here we assume the continuum limit

- Lattice spacing dependence has to be studied:
  - → found to be relatively weak for $ud\bar{c}\bar{c}$ P. Junnarkar, N. Mathur, and M. Padmanath, PRD 99, 034507 (2019)
  - → claimed as important J. Green talk at Lattice 2023

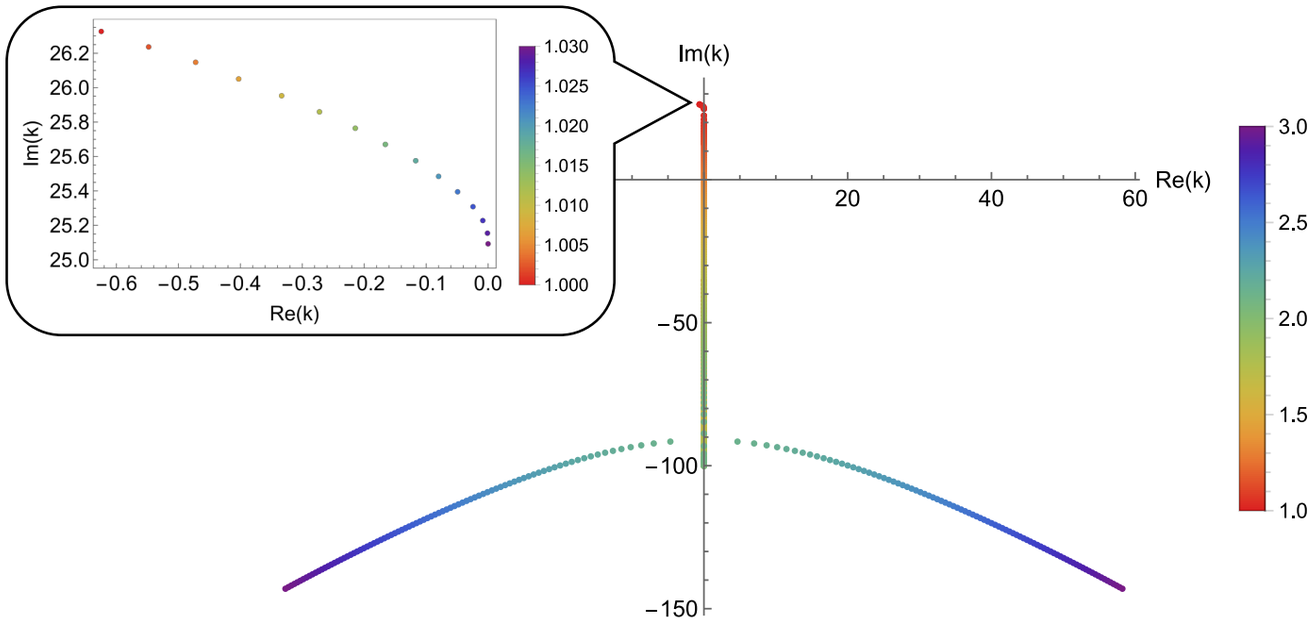
T_{cc} pole vs m_π at LO

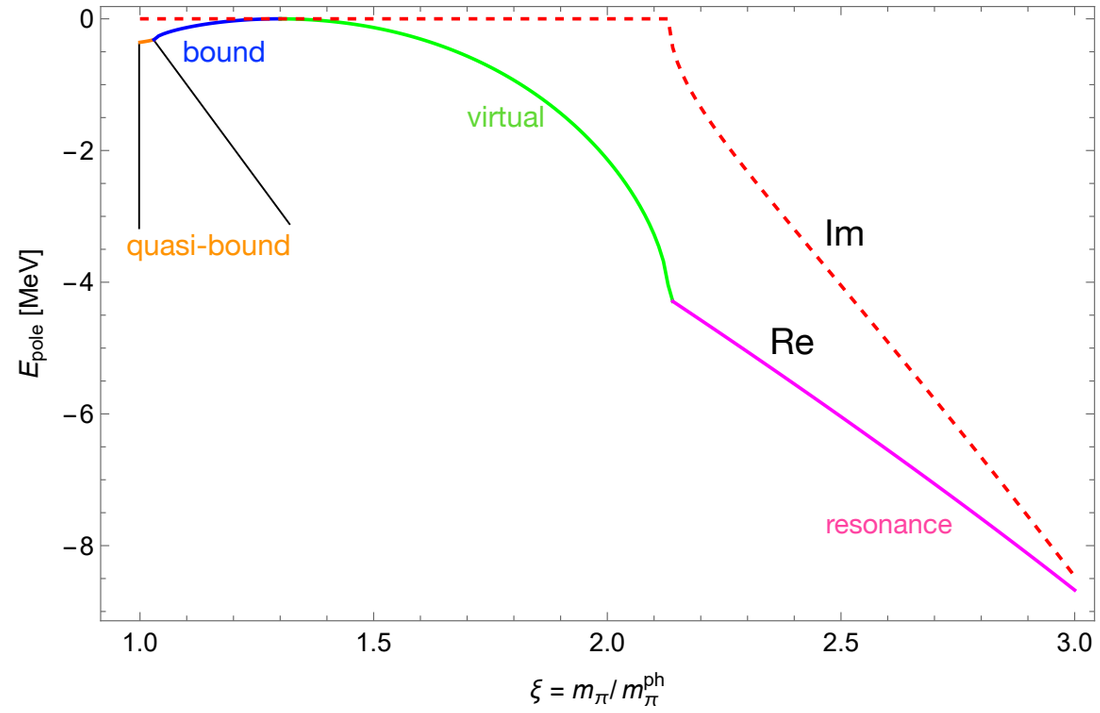
M. Abolnikov, VB, E. Epelbaum, A. Filin, C. Hanhart and L. Meng PLB 860 139188 (2025)

Fixed from the Tcc pole at physical $m_\pi^{\rm ph}$

$$V = V^{(0)}_{\rm OPE} + C^{(0)}_{^3S_1}$$

LO results





Tcc pole transitions: quasi-bound → bound → virtual → resonance

⇒ Typical trajectory for a hadronic molecule I. Matuschek, VB, F.-K. Guo, and C. Hanhart, Eur. Phys. J. A 57, 101 (2021)

Going to NLO

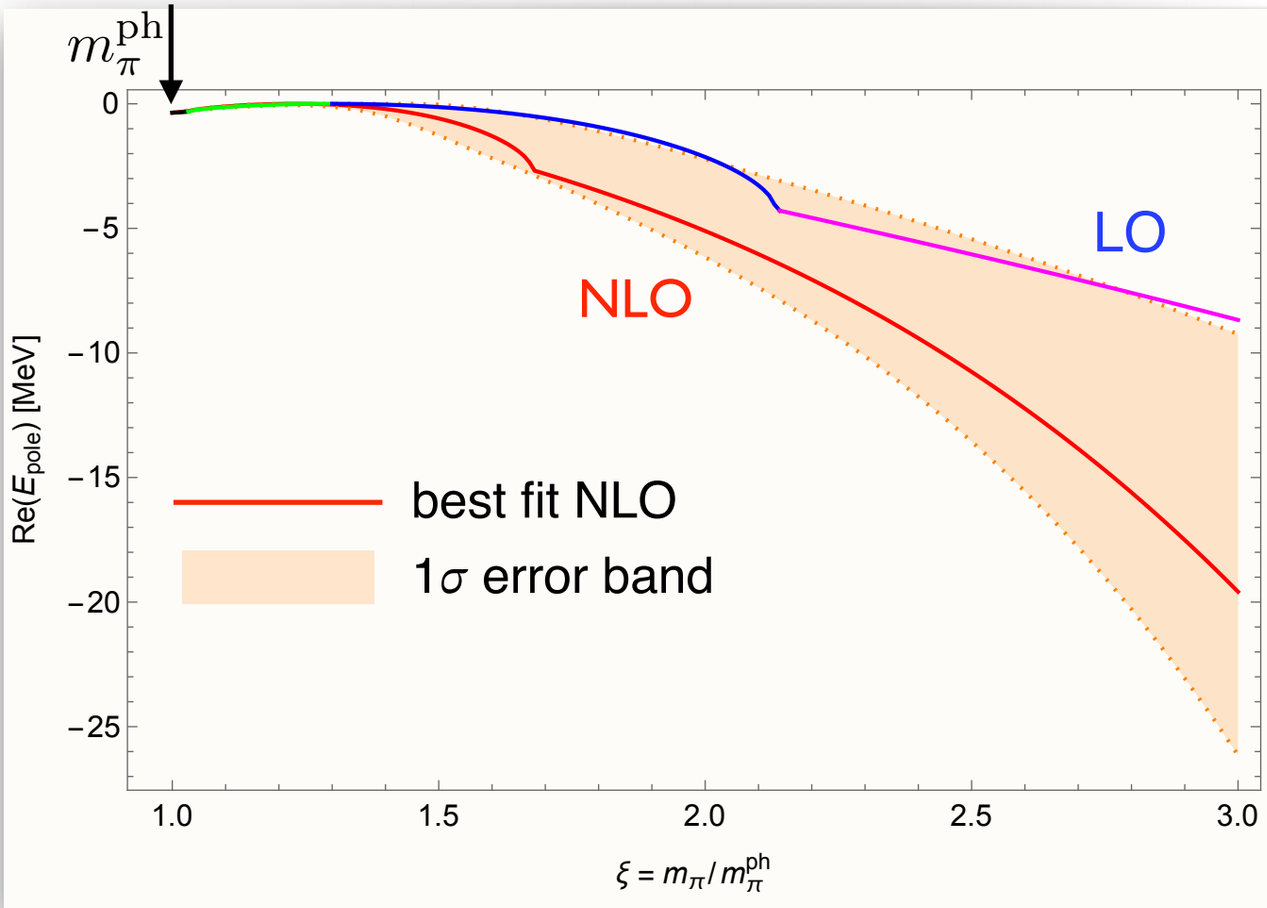
M. Abolnikov, VB, E. Epelbaum, A. Filin, C. Hanhart and L. Meng PLB 860 139188 (2025)

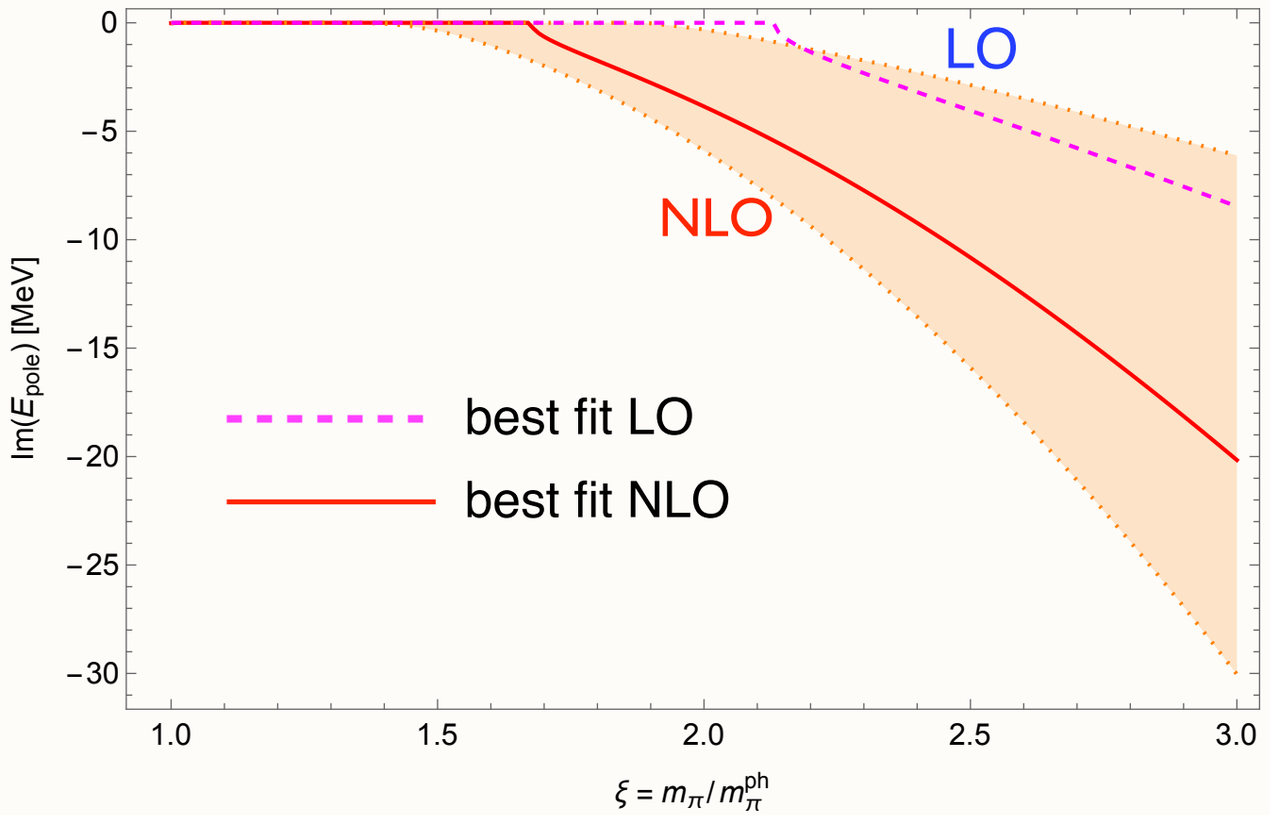
- Employ knowledge of the NLO potential at $m_\pi = m_\pi^{\rm ph}$ and $m_\pi = 280$ MeV

$$V = V^{(0)}_{\rm OPE} + V^{(0)}_{\rm cont} + V^{(2)}_{\rm cont} \qquad V^{(0)+(2)}_{\rm cont}[^3S_1] = \overline{C^{(0)}_{^3S_1}} + \overline{C^{(2)}_{^3S_1}(p^2+p'^2) + D^{(2)}_{^3S_1}(\xi^2-1)}$$

$$\xi = \frac{m_\pi}{m_\pi^{\rm ph}}$$

- Calculate scattering amplitude for any m_π



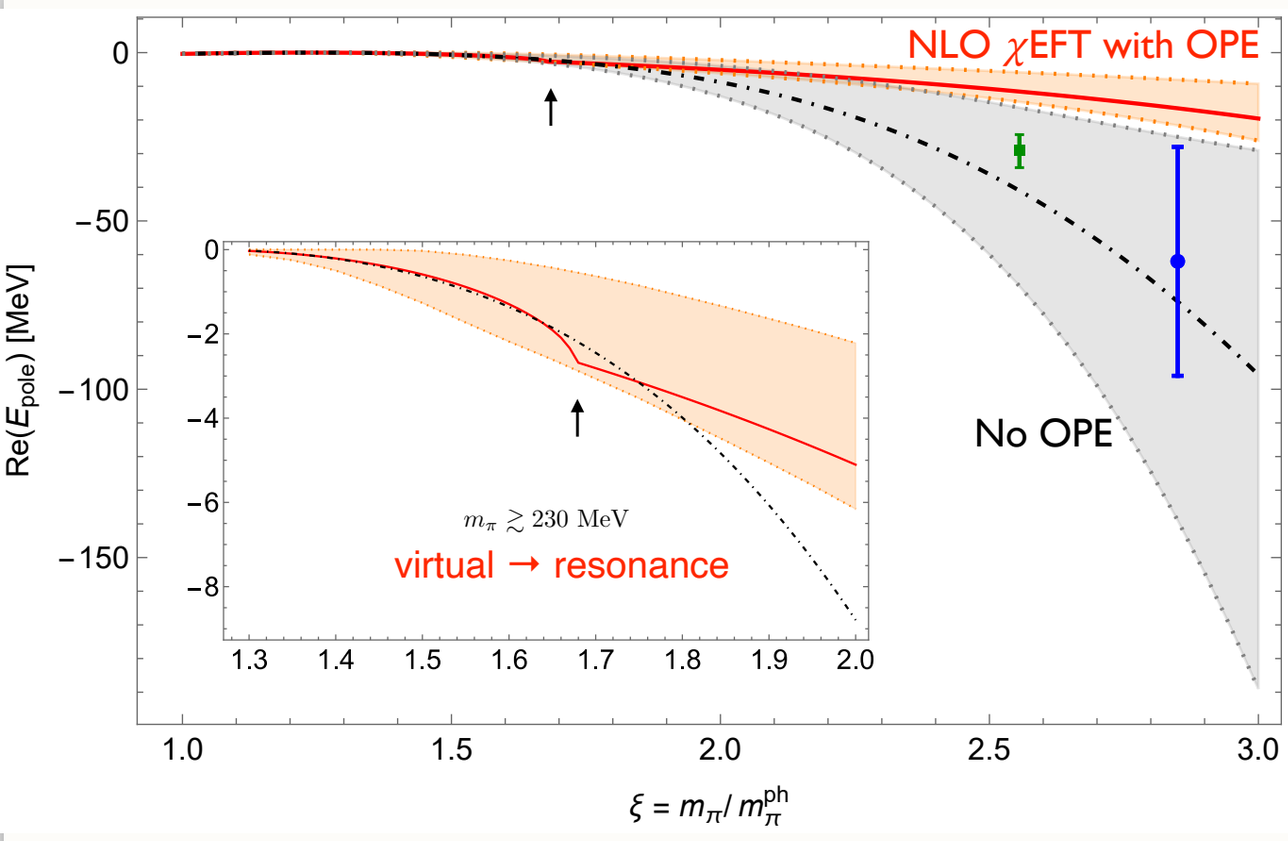


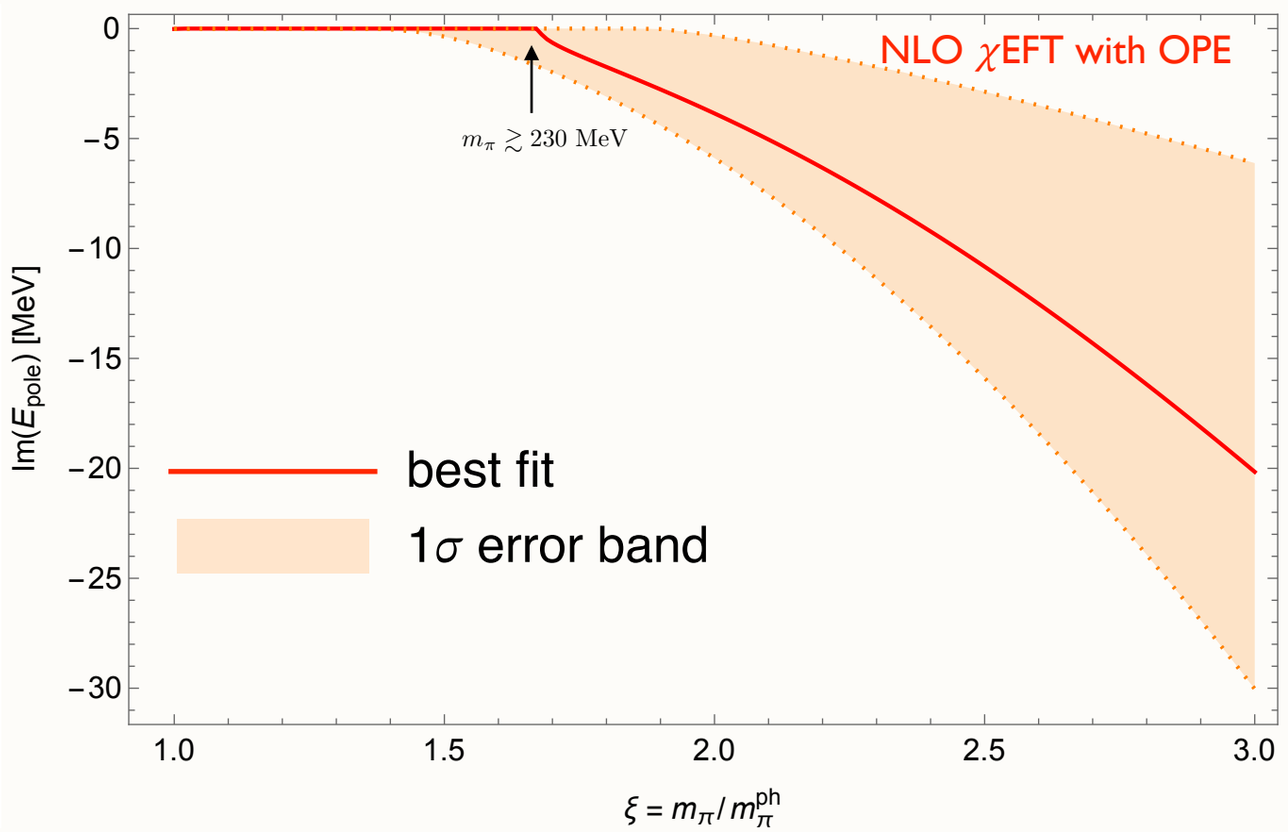
- Tcc pole transitions: quasi-bound → bound → virtual → resonance
- NLO is qualitatively consistent to LO; resonance is formed at smaller m_π
  - — systematic errors estimated conservatively: comparable/smaller than statistical

T_{cc} pole vs m_π: Contact vs Pionful

M. Abolnikov, VB, E. Epelbaum, A. Filin, C. Hanhart and L. Meng PLB 860 139188 (2025)

$$V = V^{(0)}_{\rm OPE} + V^{(0)}_{\rm cont} + V^{(2)}_{\rm cont} \qquad V^{(0)+(2)}_{\rm cont}[^3S_1] = C^{(0)}_{^3S_1} + C^{(2)}_{^3S_1}(p^2+p'^2) + D^{(2)}_{^3S_1}(\xi^2-1)$$





- Pionless EFT trajectory: virtual states for larger mpi
  - In line with Lattice: Virtual states using Lüscher + parameterization without pions

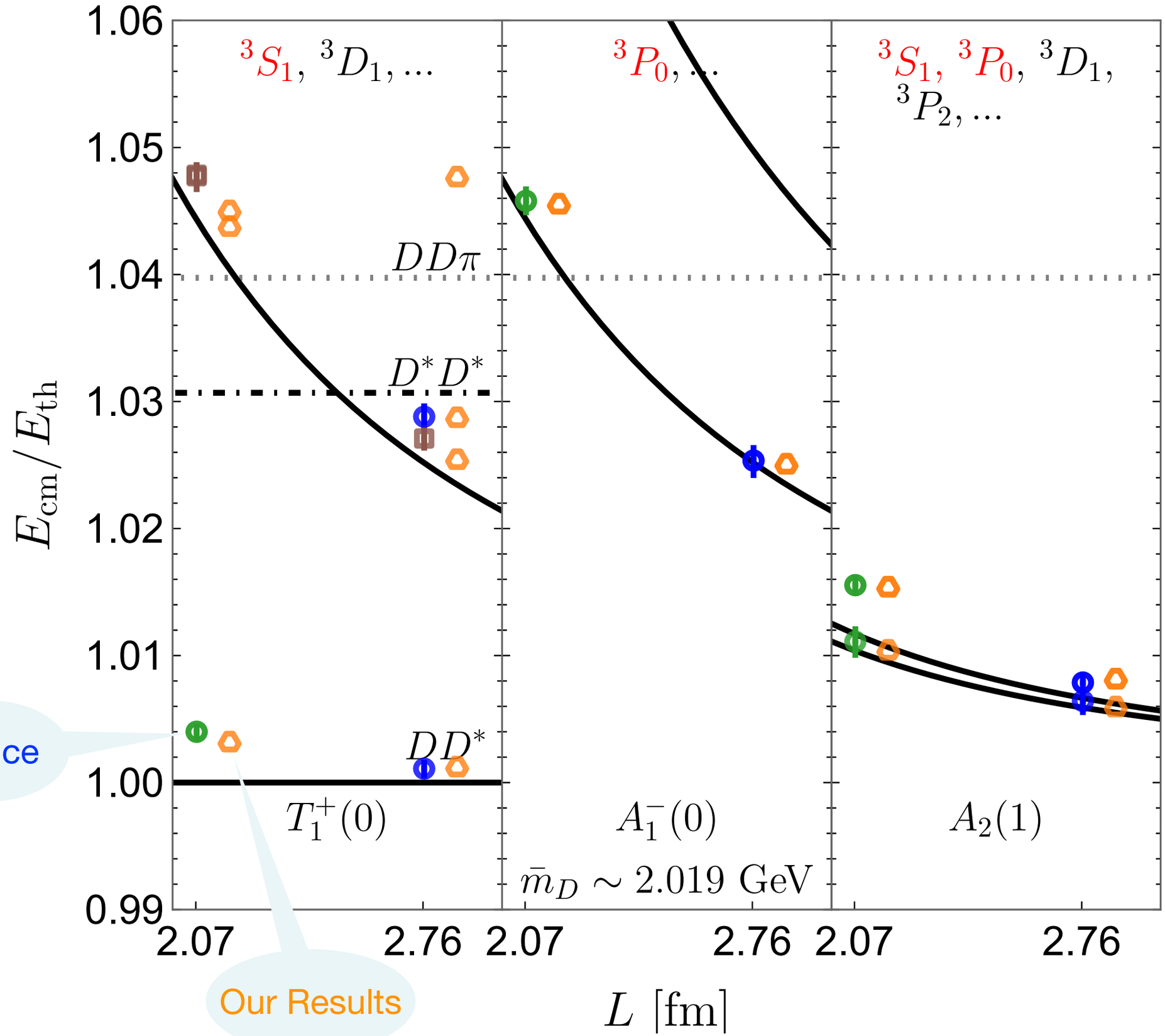
CLQCD: Chen et al. PLB 833 2022 and HadSpec: T. Whyte, D. Wilson, and C. Thomas *PRD* 111, 034511 (2025)

- But due to repulsion from the OPE, NLO χEFT yields a resonance for $m_\pi \gtrsim 230$ MeV

⇒ Long-range physics significantly changes the pole trajectory

I=1 DD* FV E-Levels at $m_\pi = 280$ MeV

Meng, Ortiz-Pacheco, VB, Epelbaum, Padmanath and Prelovsek PRD 111, 034509 (2025)



Lattice

Our Results

- Lattice
- NLO χEFT

3 Param's:

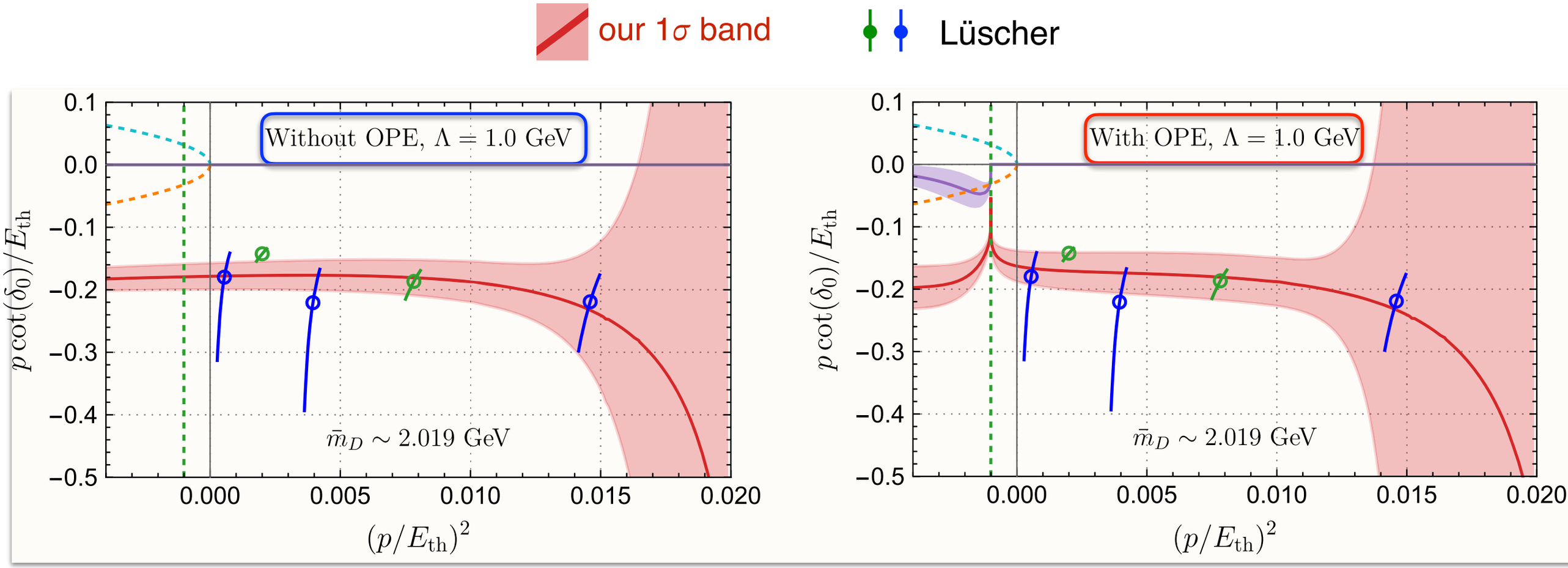
2 in $^3S_1$

1 in $^3P_0$

— OPE is included

— Repulsive interactions: datapoints are shifted upwards now

Inf. volume phase shifts: ${}^3S_1$ I=1 DD* scattering



- Repulsive interactions: no poles in the scattering amplitude near the threshold

- Effect of the OPE is weaker for I=1 than for I=0: $\langle (DD^*)_I | \boldsymbol{\tau}^{(1)} \cdot \boldsymbol{\tau}^{(2)} | (D^*D)_I \rangle_{\rm OPE} = \begin{cases} 3\ ; & I=0 \\ 1\ ; & I=1 \end{cases}$

- ${}^3S_1$ near lhc is controlled by OPE ⇒ impact the eff. range

$$a_{^3S_1} = -0.30(4)\text{fm}$$

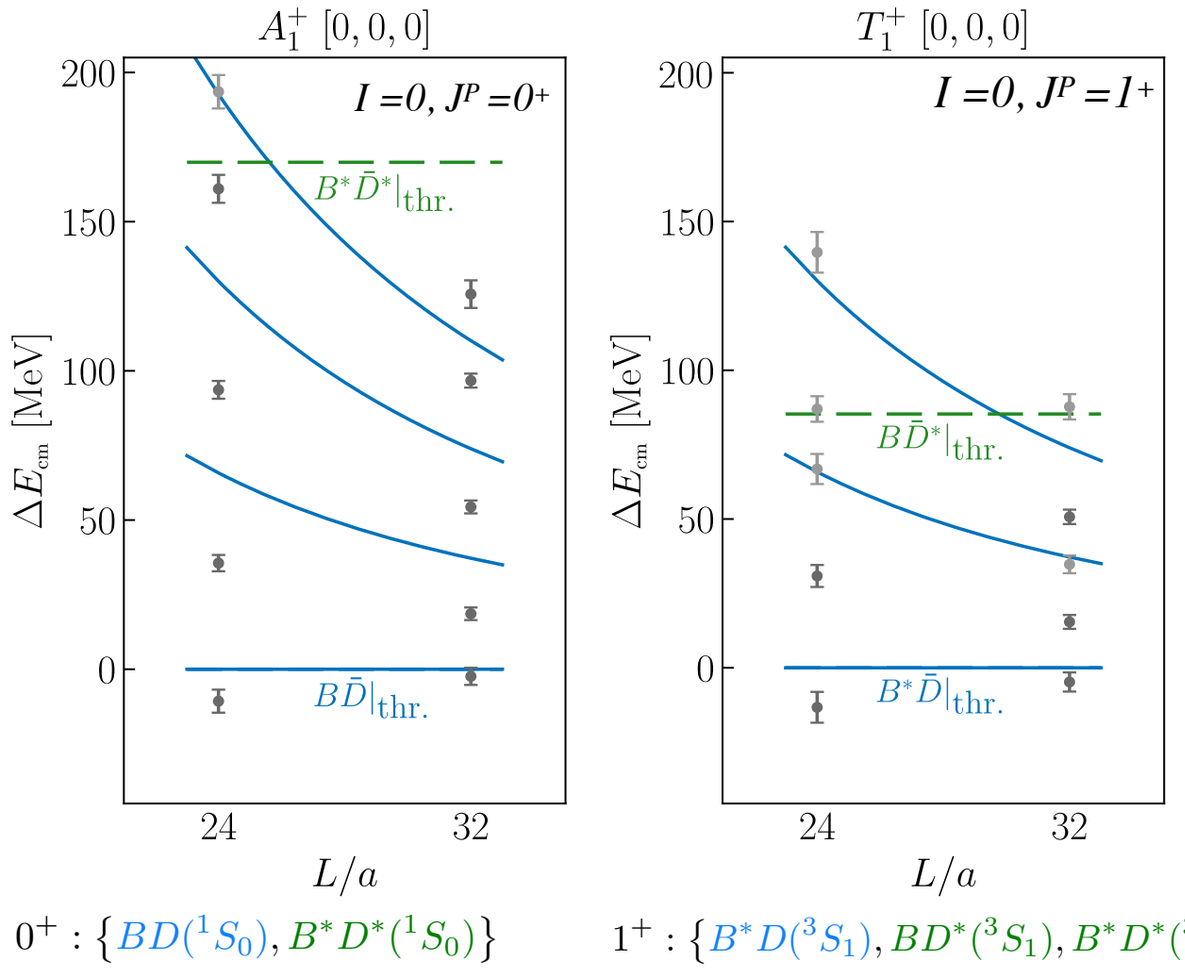
$$r_{^3S_1} = -0.89(55)\text{fm}$$

- Coupled-channel ChEFT analysis of $B^{(*)}D^{(*)}$ scattering on lattice: T_{bc}

M. Abolnikov, L. Meng, VB, E. Epelbaum, A. Filin, A. Gasparyan PRD **113**, 114041 (2026), arXiv:2602.02176 [hep-ph]

T_{bc} from lattice QCD in finite volume $\bar{b}\bar{c}qq$

$m_\pi \simeq 220$ MeV, $a \simeq 0.12$ fm



$0^+ : \{BD(^1S_0), B^*D^*(^1S_0)\}$ $\quad$ $1^+ : \{B^*D(^3S_1), BD^*(^3S_1), B^*D^*(^3S_1)\}$

Alexandrou, Finkenrath, Leontiou, Meinel, Pflaumer, Wagner , PRL 132, 151902 (2024)

- Lüscher analysis of EFV for BD (J=0) and B*D (J=1)
- ERE analysis of the extracted phase shifts:

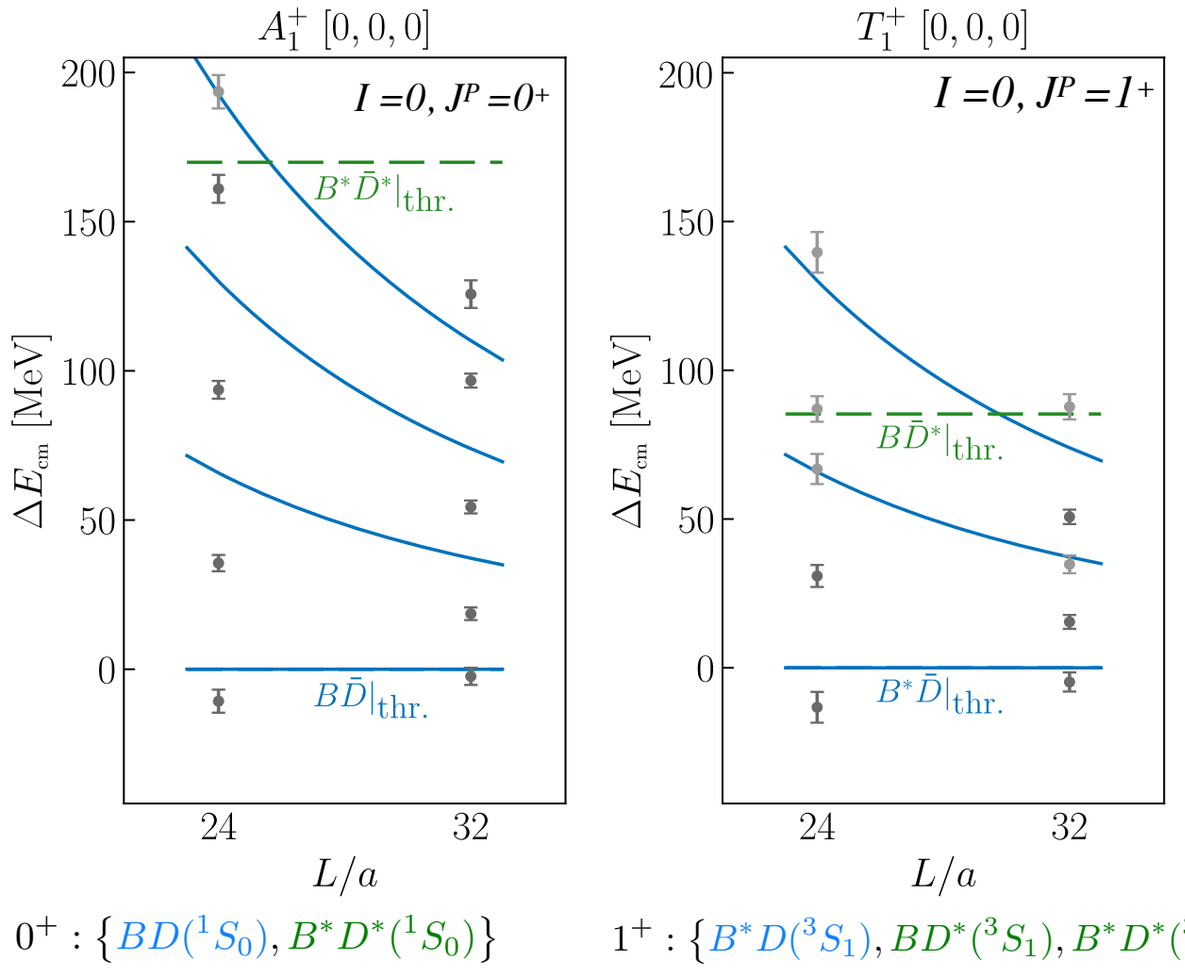
— Two shallow bound T_{bc} states: $E_B \sim 1$ MeV

— Hints for broad resonances ~100 MeV above thr.

- Not included: OPE, coupled-channels, HQ symmetry

T_{bc} from lattice QCD in finite volume $\bar{b}\bar{c}qq$

$m_\pi \simeq 220$ MeV, $a \simeq 0.12$ fm



$0^+ : \{BD(^1S_0), B^*D^*(^1S_0)\}$ $\quad$ $1^+ : \{B^*D(^3S_1), BD^*(^3S_1), B^*D^*(^3S_1)\}$

Alexandrou, Finkenrath, Leontiou, Meinel, Pflaumer, Wagner , PRL 132, 151902 (2024)

- Lüscher analysis of EFV for BD (J=0) and B*D (J=1)
- ERE analysis of the extracted phase shifts:
  - Two shallow bound T_{bc} states: $E_B \sim 1$ MeV
  - Hints for broad resonances ~100 MeV above thr.
- Not included: OPE, coupled-channels, HQ symmetry

Coupled-channel EFT to NLO:

Abolnikov, VB, et al. arXiv:2602.02176 [hep-ph]

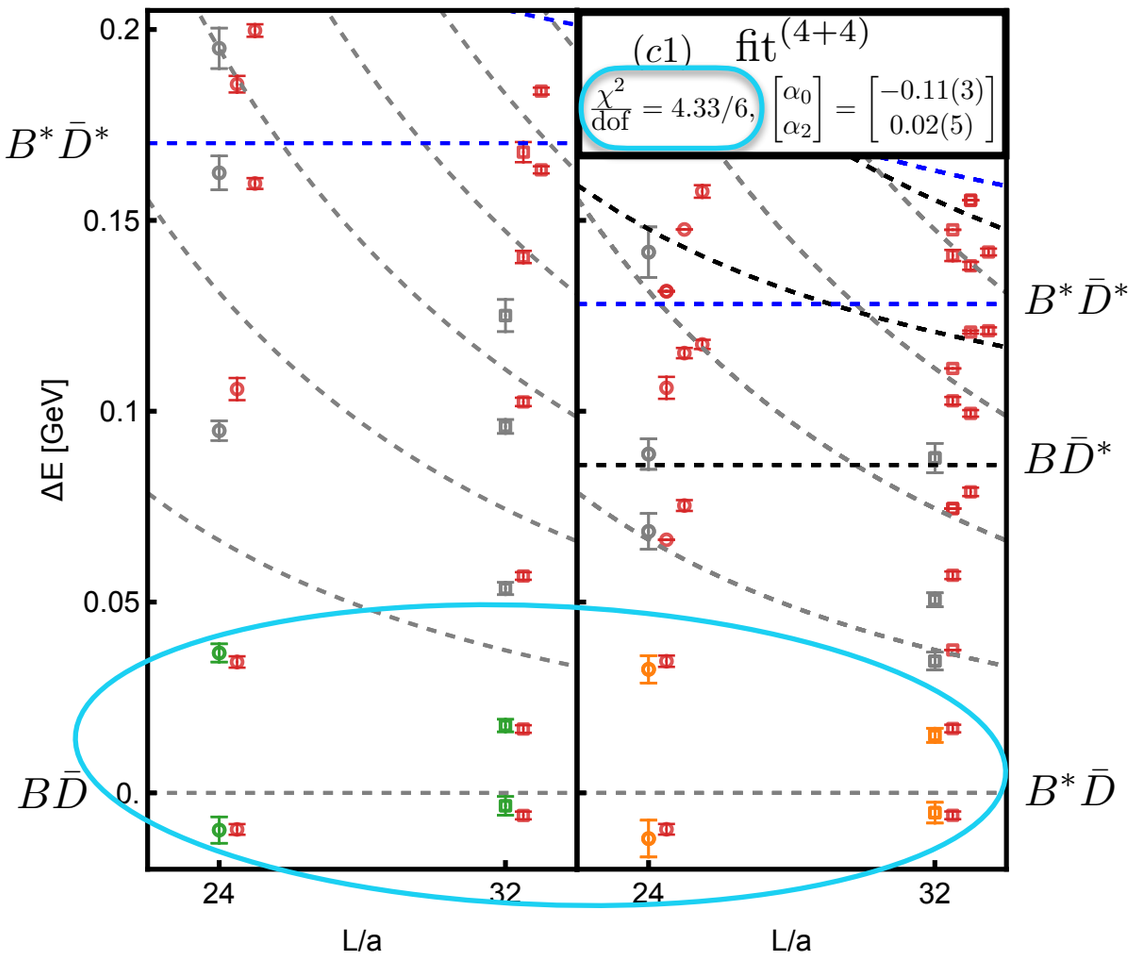
- HQSS: LO contact potentials for $J^P = 0^+, 1^+, 2^+$ depend of two parameters C_d and C_f

- Lowest channels: EFV receive OPE effects only from off-diag. transitions

$$V^{(0)}_{\rm OPE}[0^+] = \begin{pmatrix} 0 & V^{B\bar{D}\to B^*\bar{D}^*}_{\rm OPE} \\ V^{B^*\bar{D}^*\to B\bar{D}}_{\rm OPE} & V^{B^*\bar{D}^*\to B^*\bar{D}^*}_{\rm OPE} \end{pmatrix} \qquad V^{(0)}_{\rm OPE}[1^+] = \begin{pmatrix} 0 & V^{B^*\bar{D}\to B\bar{D}^*}_{\rm OPE} & V^{B^*\bar{D}\to B^*\bar{D}^*}_{\rm OPE} \\ V^{B\bar{D}^*\to B^*\bar{D}}_{\rm OPE} & 0 & V^{B^*\bar{D}\to B^*\bar{D}^*}_{\rm OPE} \\ V^{B^*\bar{D}^*\to B^*\bar{D}}_{\rm OPE} & V^{B^*\bar{D}^*\to B\bar{D}^*}_{\rm OPE} & V^{B^*\bar{D}^*\to B^*\bar{D}^*}_{\rm OPE} \end{pmatrix}$$

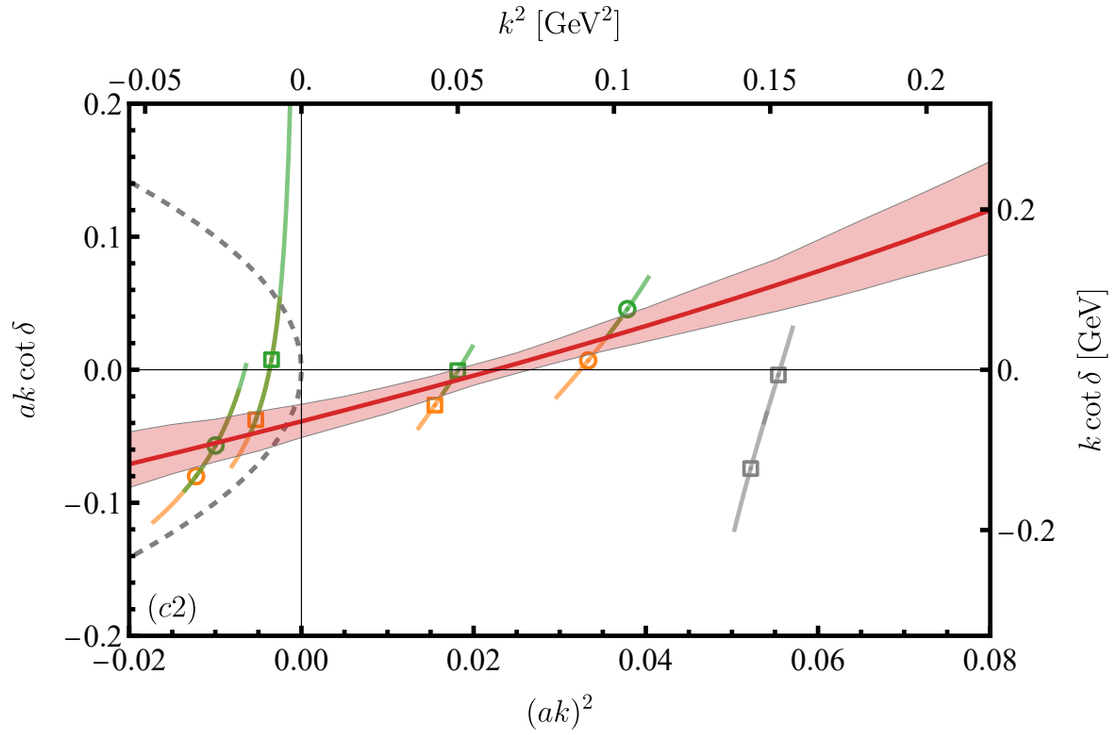
No diagonal OPE in contrast to Tcc!

EFT I: Single channel at low energies



- Focus only on the low-energy states
- Integrate out higher channels

⇒ Single-channel pure contact EFT: $V_{\text{cont}} = \mathcal{C}_d + \mathcal{D}_d(p^2 + p'^2)$



HQSS consequence: $V[B\bar{D}] = V[B^*\bar{D}] = V[B\bar{D}^*]$

⇒ States in $A_1^+[0]$ and $T_1^+[0]$ are in excellent agreement with HQSS

Pole positions

Channel	J^P	EFT1	Alexandrou et al.	
$B\bar{D}$	0^+	$-1.8^{+1.0+1.6}_{-1.3-4.0}$	$-0.5^{+0.4}_{-1.5}$	} Consistent results
$B^*\bar{D}$	1^+	$-1.7^{+0.9+1.6}_{-1.3-4.0}$	$-2.4^{+2.0}_{-0.7}$	
$B\bar{D}^*$	1^+	$-3.6^{+1.2+2.7}_{-1.5-5.0}$	—	} There must be other states based on HQSS
$B^*\bar{D}^{*\dagger}$	$0^+, 1^+, 2^+$	$-3.6^{+1.2+2.7}_{-1.5-5.0}$	—	

EFT2: Coupled-channel for all available data

- Fits to all (9+5) data by gradually increasing complexity

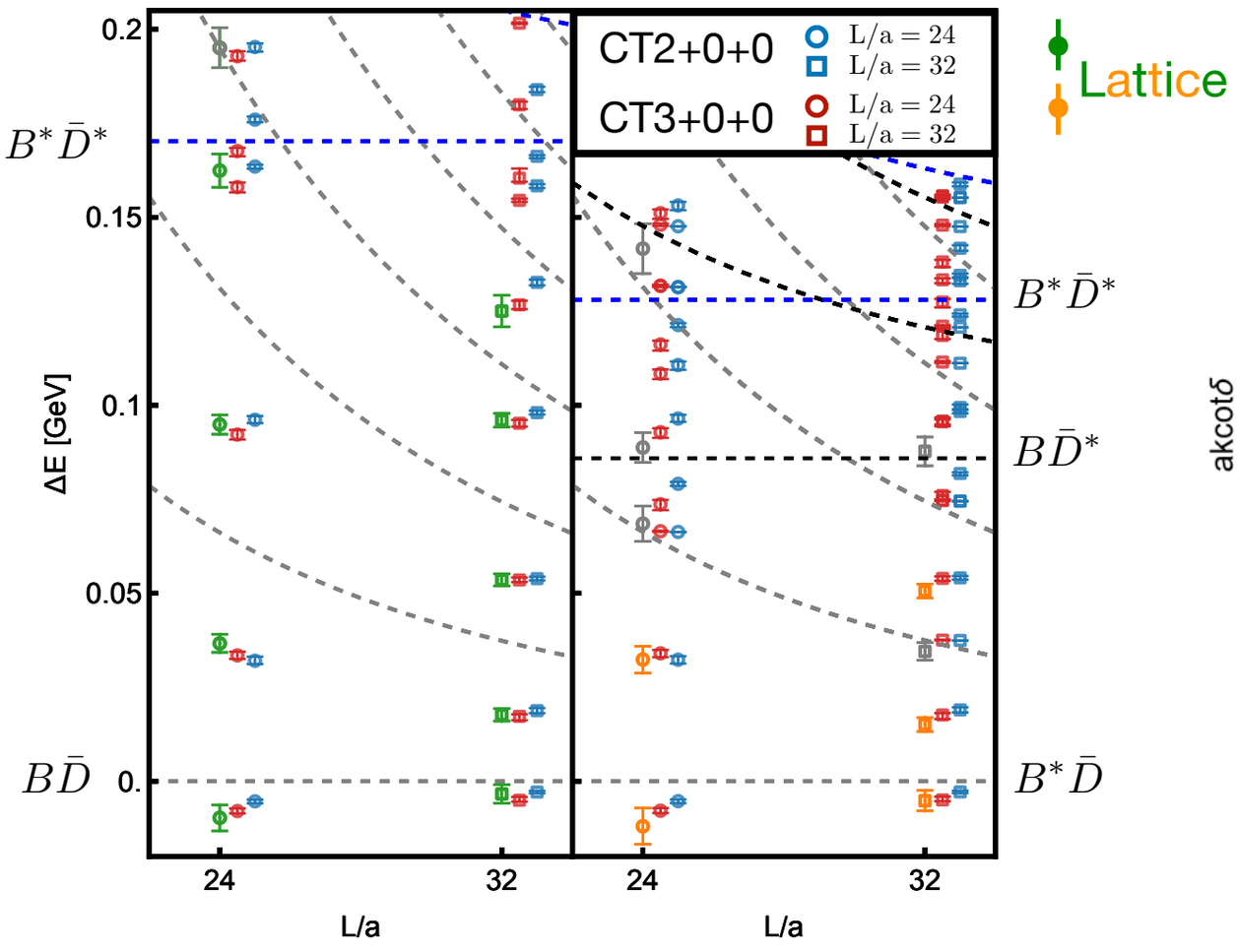
  1. Single-channel fit: $V_{\rm cont} = \mathcal{C}_d + \mathcal{D}_d(p^2 + p'^2)$

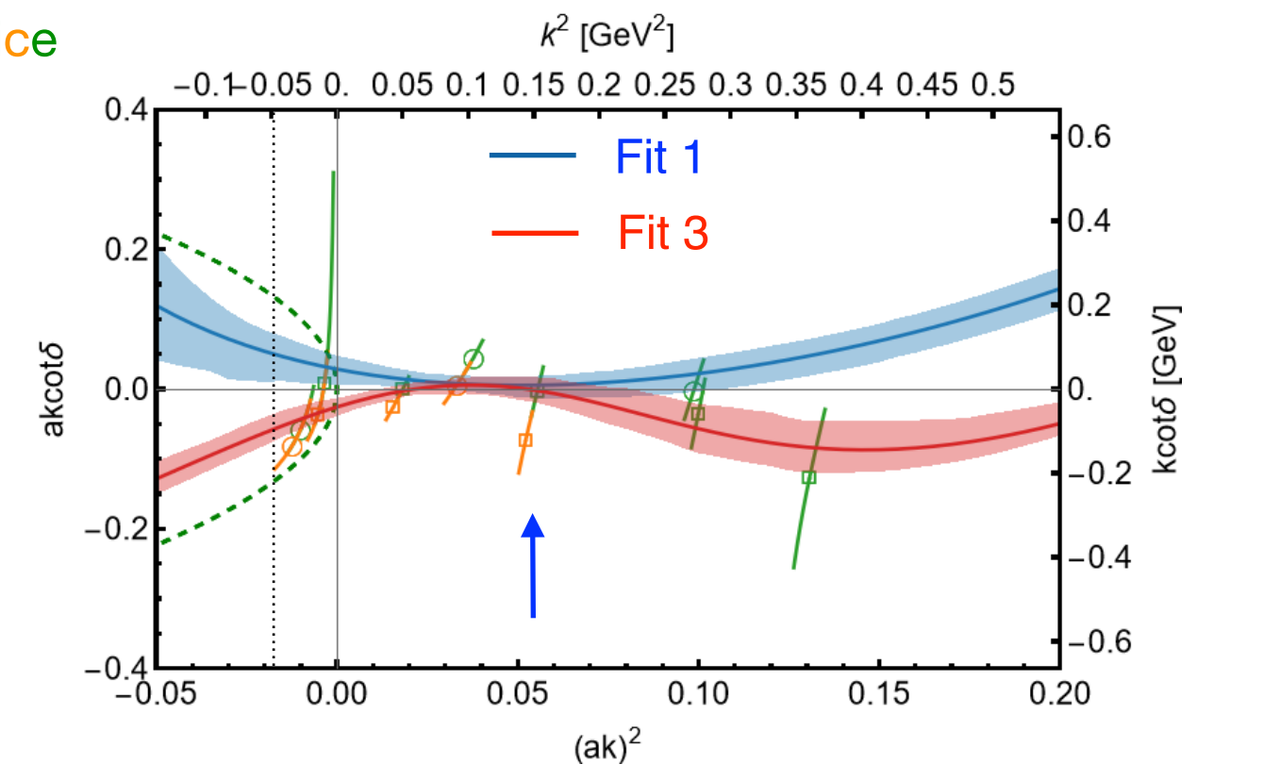
  2. Coupled-channel fit: off diag. C_f and OPE included in addition

  3. Single-channel fit: $V_{\rm cont} = \mathcal{C}_d + \mathcal{D}_d(p^2 + p'^2) + \mathcal{E}_d(p^4 + p'^4)$

$\frac{\chi^2}{\rm dof}$	
$\frac{22.1}{12}$	
$\frac{16.9}{11}$	⇒ Improves but not much, weak cc
$\frac{8.8}{11}$	⇒ Big improvement

Fit 3 vs Fit 1





- Significant improvement for ground states
- Consistent with the normal distributions
- Data change the trend starting from the 5 datapoint

⇒ captured by $\mathcal{E}_d(p^4 + p'^4)$

Quantile-Quantile Plots: EFT I

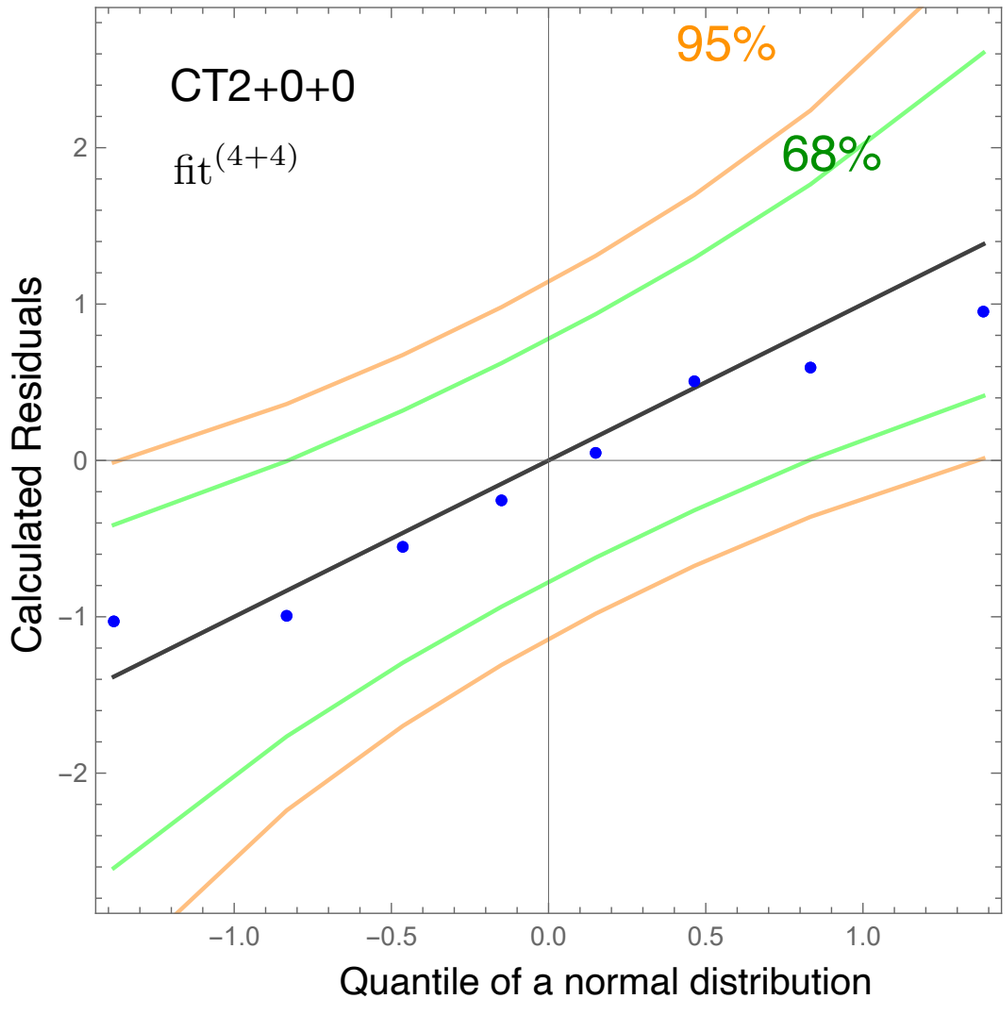
- Test “normality” of the theory

$$\chi^2(\{\mathcal{C}_{\rm cont}\}) = \sum_{i,j} \delta E(i,\{\mathcal{C}_{\rm cont}\}) C^{-1}(i,j) \delta E(j,\{\mathcal{C}_{\rm cont}\})$$

CT2+0+0 $\quad V_{\rm cont} = \mathcal{C}_d + \mathcal{D}_d(p^2 + p'^2)$

$$\delta E(i,\{\mathcal{C}_{\rm cont}\}) = E^{\rm LQCD}(i) - E^{\rm EFT}(i,\{\mathcal{C}_{\rm cont}\})$$

$$\mathrm{Res}_i = \frac{E^{\rm EFT}(i) - E^{\rm LQCD}(i)}{\Delta E^{\rm LQCD}(i)}$$

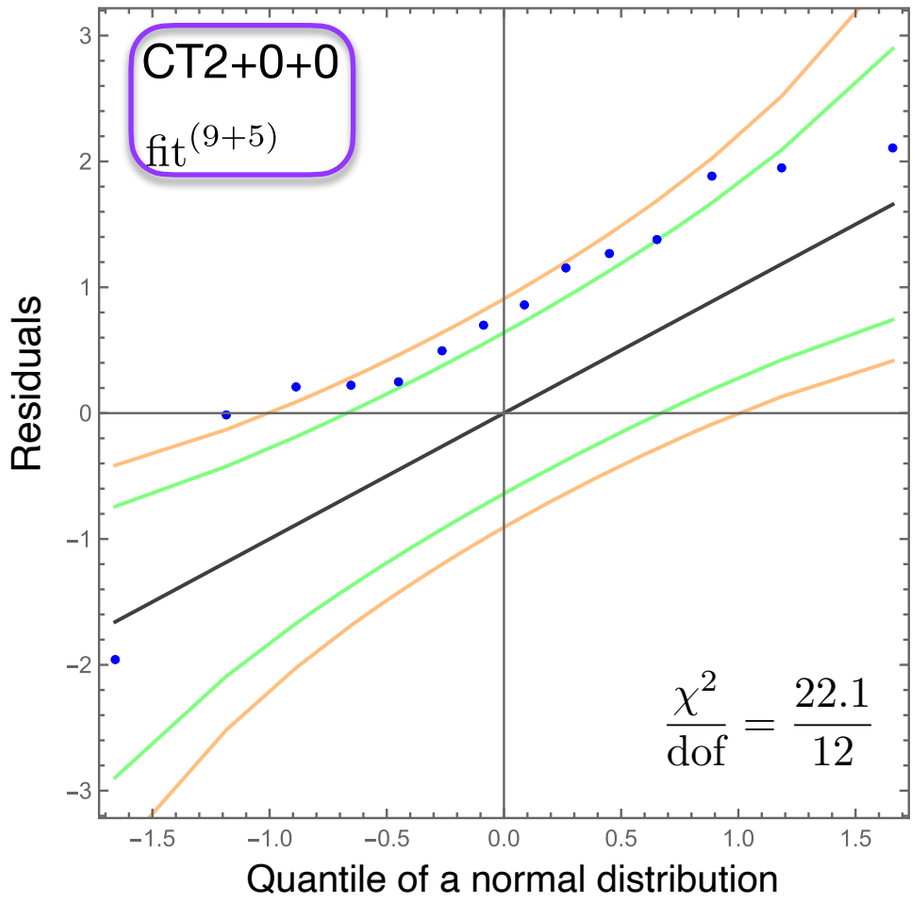


⇒ Nearly normal

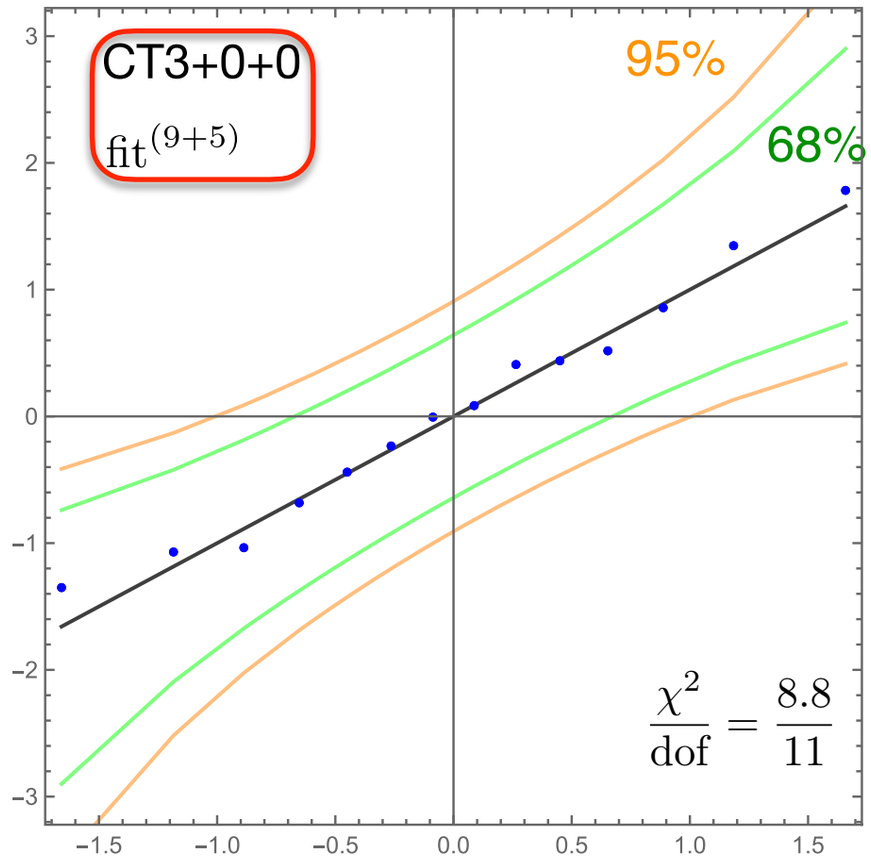
Quantile-Quantile Plots: EFT2

- Consistency check: theory vs normal distribution

$V_{\rm cont} = \mathcal{C}_d + \mathcal{D}_d(p^2 + p'^2)$



$V_{\rm cont} = \mathcal{C}_d + \mathcal{D}_d(p^2 + p'^2) + \mathcal{E}_d(p^4 + p'^4)$



x = y line:	strong deviations	closely follow
68% band:	many data points fall above	all data points within
95% band:	some beyond	all within
	⇒ Not normal	⇒ Normal

T_{bc} : pole positions and conclusions

Channel	J^P	RS	EFT1(CT2+0+0) Poles [MeV]	EFT2(CT3+0+0) Poles [MeV]	Alexandrou et al. Poles [MeV]
$B\bar{D}$	0^+	(+)	$-1.8^{+1.0+1.6}_{-1.3-4.0}$	$-0.8^{+0.6+0.4}_{-1.1-0.6}$	$-0.5^{+0.4}_{-1.5}$
$B^*\bar{D}$	1^+	(+)	$-1.7^{+0.9+1.6}_{-1.3-4.0}$	$-0.7^{+0.6+0.4}_{-1.0-0.6}$	$-2.4^{+2.0}_{-0.7}$
$B\bar{D}^*$	1^+	(+)	$-3.6^{+1.2+2.7}_{-1.5-5.0}$	$-8.0^{+2.8+1.3}_{-3.4-1.4}$	—
$B^*\bar{D}^{*\dagger}$	$0^+, 1^+, 2^+$	(+)	$-3.6^{+1.2+2.7}_{-1.5-5.0}$	$-7.6^{+2.7+1.3}_{-3.3-1.4}$	—

EFT confirms shallow Tbc states!

Compositeness ~ 0.9

⇒ molecules

- Lowest-channel poles are mutually consistent and agree with lattice results.
- Data respect HQSS → expect partner states near higher thresholds.
- Broad resonance poles are artefacts (outside EFT validity).
- Best-fit: (i) small coupled-channel effects (ii) OPE has little impact on the lowest states

But: —OPE is diagonal in B*D* ⇒ stronger impact expected

—Alternative fit with sizable off diag transitions ~D_f : but larger χ^2 and non-normal residuals

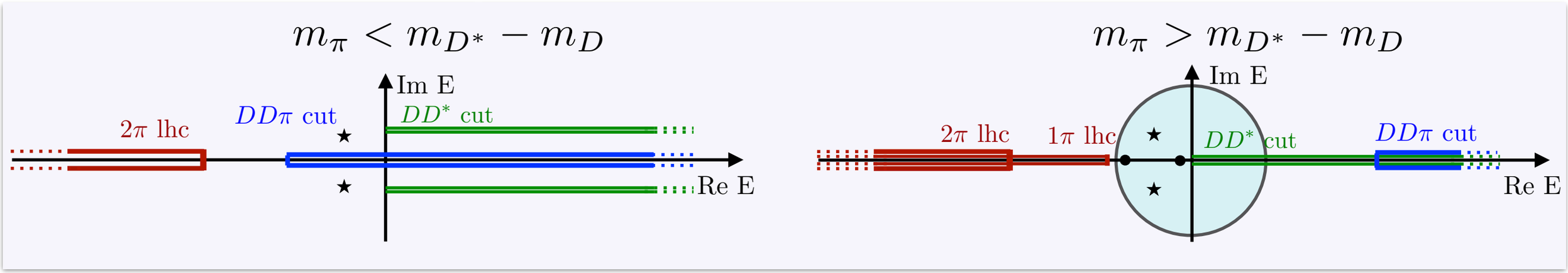
⇒ Key probe: lattice data in the higher channels!

Summary and Conclusions

- Unitarity- and analyticity-preserving extraction of exotic state properties
- χEFT is well suited for analysing data in the infinite and finite volume

Other FV methods: Dawid, Romero-Lopez, Sharpe *JHEP* (2025); Raposo, Hansen *JHEP* (2024);
see talk by Wu Jia-Jun on Thursday Bubna et al. JHEP (2024); Hansen et al. JHEP (2024), ….

- Long-range interaction: important in low-energy DD* scattering



but less pronounced for $B^{(*)}D$ scattering B^*D^*?

- Chiral extrapol's of the T_{cc} and T_{bc} states

Lattice studies at different m_π + discretisation errors on lattice

The role of coupled channels? Data near higher thresholds!

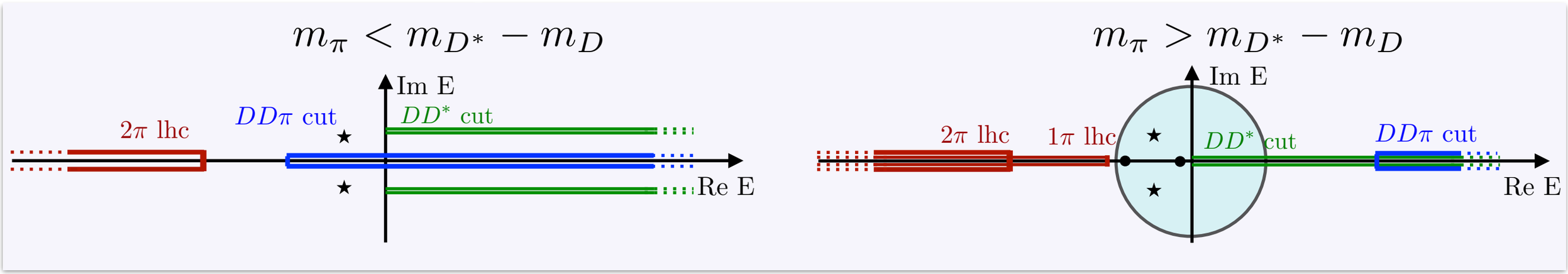
Consequences of HQSS: spin partner(s) on lattice

Summary and Conclusions

- Unitarity- and analyticity-preserving extraction of exotic state properties
- χEFT is well suited for analysing data in the infinite and finite volume

Other FV methods: Dawid, Romero-Lopez, Sharpe *JHEP* (2025); Raposo, Hansen *JHEP* (2024);
see talk by Wu Jia-Jun on Thursday Bubna et al. JHEP (2024); Hansen et al. JHEP (2024), ….

- Long-range interaction: important in low-energy DD* scattering



but less pronounced for $B^{(*)}D$ scattering B^*D^*?

- Chiral extrapol's of the T_{cc} and T_{bc} states

Lattice studies at different m_π + discretisation errors on lattice

The role of coupled channels? Data near higher thresholds!

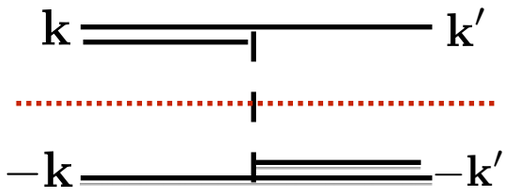
Consequences of HQSS: spin partner(s) on lattice

Thank you!

Backup

Left-Hand Cut

— Leading singularity is from the on shell one-pion exchange



PWD of the static potential:

$$V_{l=0}(k,k') \propto \int dz \frac{1}{(\mathbf{k}-\mathbf{k}')^2+\mu^2} = \frac{1}{2kk'} \log \frac{(k+k')^2+\mu^2}{(k-k')^2+\mu^2} \xrightarrow[k=k'=p]{\text{on shell}} \frac{1}{2p^2} \log \frac{4p^2+\mu^2}{\mu^2}$$

$\Rightarrow$ left-hand cut (lhc) branch point is at

$$(p^{1\pi}_{\rm lhc})^2 = -\frac{\mu^2}{4}$$

For DD*

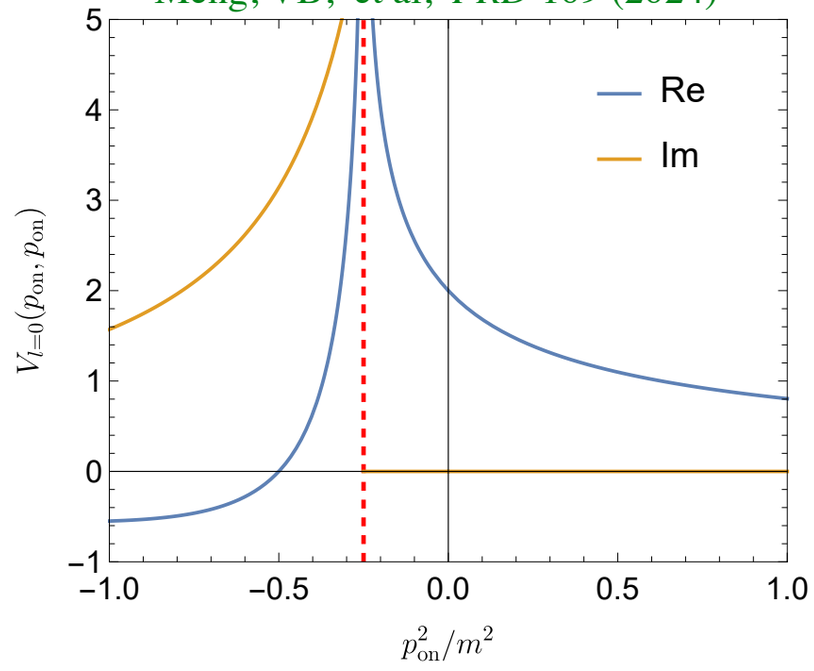
$\mu^2 = m_\pi^2 - \Delta M^2$

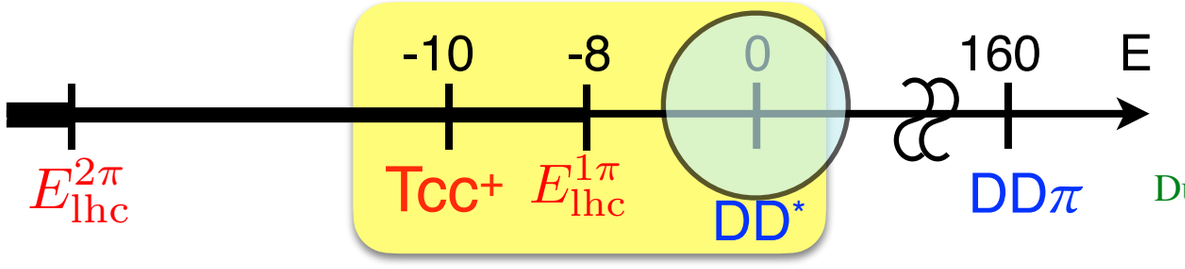
$\Delta M = m_{D^*} - m_D$

Sc. amplitude is complex for E below the lhc
$\Rightarrow$ Lüscher's method breaks down

Raposo and Hansen 2311.18793 (2023), Green et al, *PRL* 127 (2021) , Meng et al, *PRD* 109 (2024)

Meng, VB, et al, *PRD* 109 (2024)





$\Rightarrow$ ERE is only applicable until lhc

Du, Filin, VB, Dong, Epelbaum, Guo, Hanhart, Nefediev, Nieves, Wang *PRL* 131 (2023)

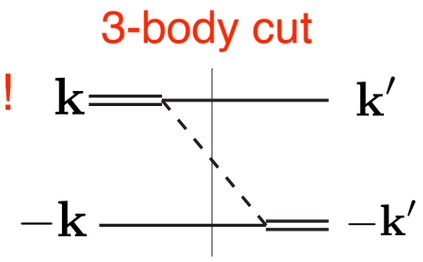
3-body DDπ cut

- OPE potential:

$$V_{\mathrm{DD}^*\to\mathrm{DD}^*}(\mathbf{k},\mathbf{k}',E)\propto\frac{g_c^2}{(4\pi f_\pi)^2}\,\tau_1\cdot\tau_2\,\frac{(\epsilon_1\cdot\vec{q})\,(\epsilon_2'^{\,*}\cdot\vec{q})}{2E_\pi(\mathbf{k}-\mathbf{k}')}\left(\frac{1}{D_{DD\pi}(\mathbf{k},\mathbf{k}',E)}+\frac{1}{D_{D^*D^*\pi}(\mathbf{k},\mathbf{k}',E)}\right)$$

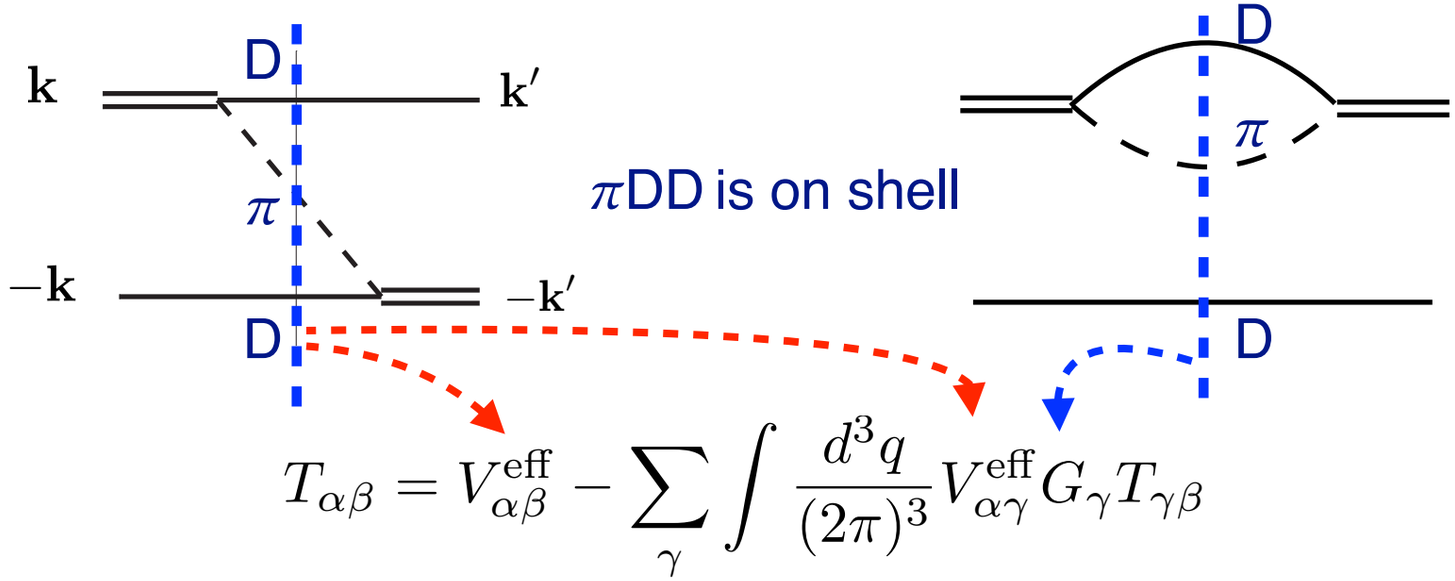
$$D_{DD\pi}(k,k',E)=E_D(k)+E_D(k')+E_\pi(\mathbf{k}-\mathbf{k}')-E$$

goes on shell! $\Rightarrow$



$$D_{DD\pi}(k,k',E)\to i\pi\delta(E_D(k)+E_D(k')+E_\pi(\mathbf{k}-\mathbf{k}')-E)\to\text{Im part}$$

- 3-body cut stems from OPE potential and self energies in the Green function



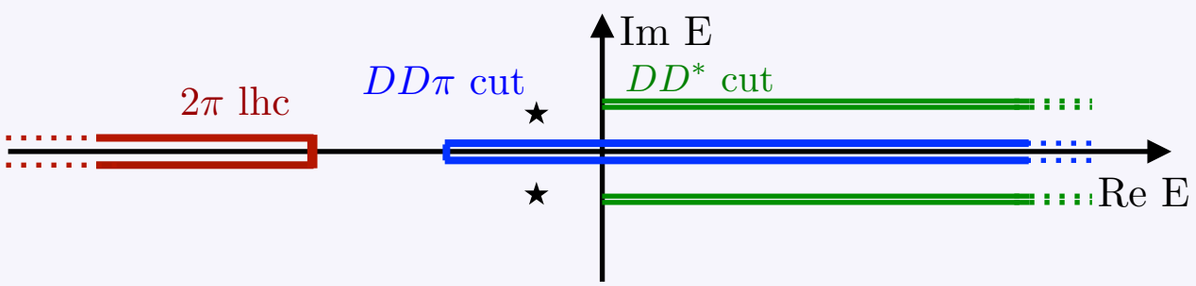
Bose statistics for DD requires both cont's to appear together

- Scattering amplitude and its poles acquire an Im part

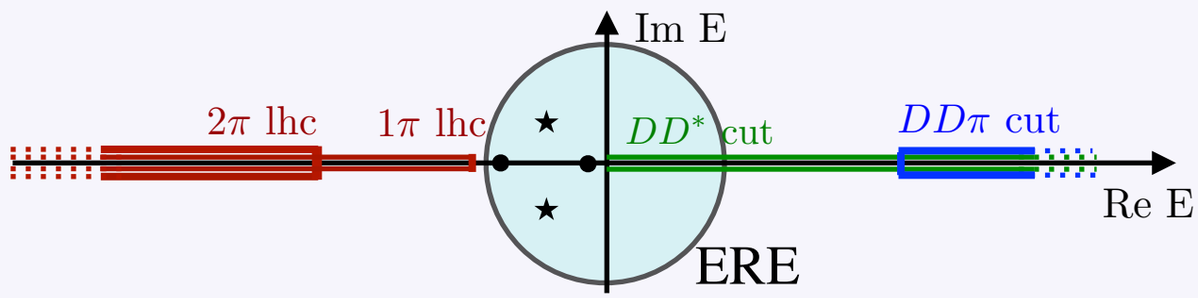
Analytic structure of the DD* scatt. ampl. : Summary

– Cut structure depends on the (light-quark or) pion mass

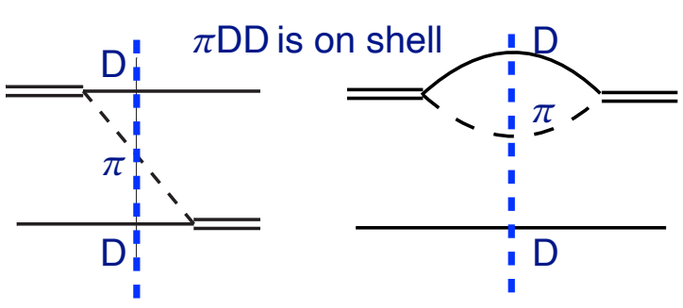
Real world: $m_\pi < m_{D^*} - m_D$



Lattice: $m_\pi > m_{D^*} - m_D$



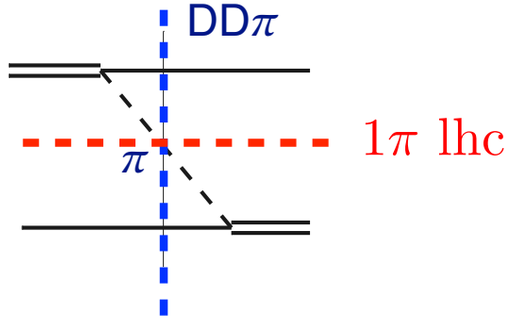
3-body DDπ cut



⇒ Prominent role for the T_{cc} width

M. Du, VB, et al *PRD* 105, 014024 (2022)

Left-hand cuts



⇒ Constraints on the ERE applicability range

M. Du, VB et al, *PRL* 131, 131903 (2023)

⇒ Invalidate Lüscher's QC at least below lhc

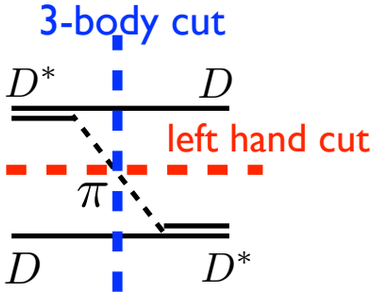
Green et al (2021), Raposo and Hansen (2023),
Dawid et al. (2023), Meng, VB et al (2023), …

– The leading nearby cut is always associated with the one-pion exchange (OPE)

⇒ Theoretical framework has to include it!

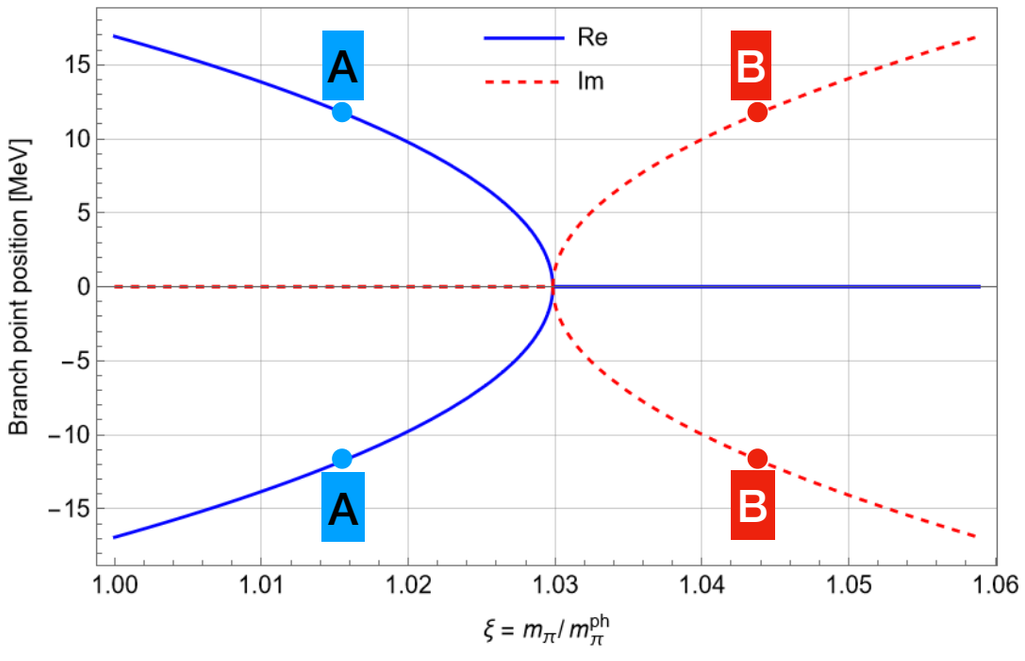
Cuts in the on-shell partial-wave projected OPE potential

M. Abolnikov, VB, E. Epelbaum, A. Filin, C. Hanhart and L. Meng PLB 860 139188 (2025)



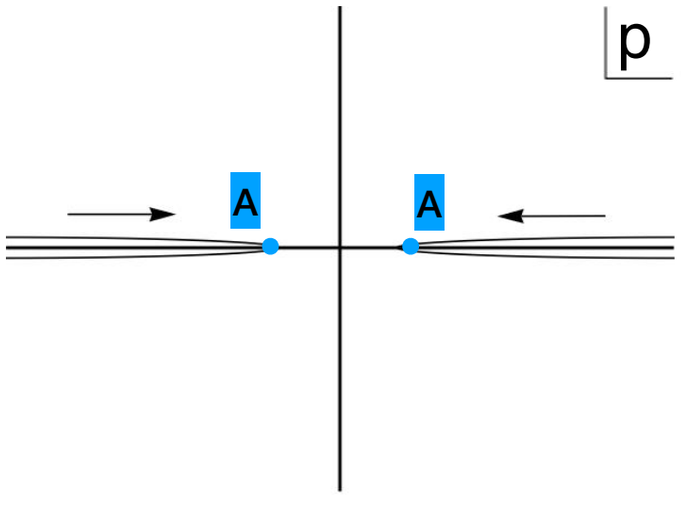
$$V_{\mathrm{l}=0}(k,k',E) \propto \log\left(\frac{\sqrt{(k+k')^2+m_\pi^2}-\Delta M+\frac{k^2+k'^2}{2m}-\frac{p^2}{2\mu}-i\epsilon}{\sqrt{(k-k')^2+m_\pi^2}-\Delta M+\frac{k^2+k'^2}{2m}-\frac{p^2}{2\mu}-i\epsilon}\right) \xrightarrow[k=k'=p]{\text{on shell}} \log\left(\frac{\sqrt{4p^2+m_\pi^2}-\Delta M+\frac{p^2}{m}-\frac{p^2}{2\mu}-i\epsilon}{m_\pi-\Delta M+\frac{p^2}{m}-\frac{p^2}{2\mu}-i\epsilon}\right)$$

$$\Delta M = m_{D^*}-m_D \qquad \mu=\frac{m_{D^*}m_D}{m_{D^*}+m_D} \qquad m\equiv m_D$$



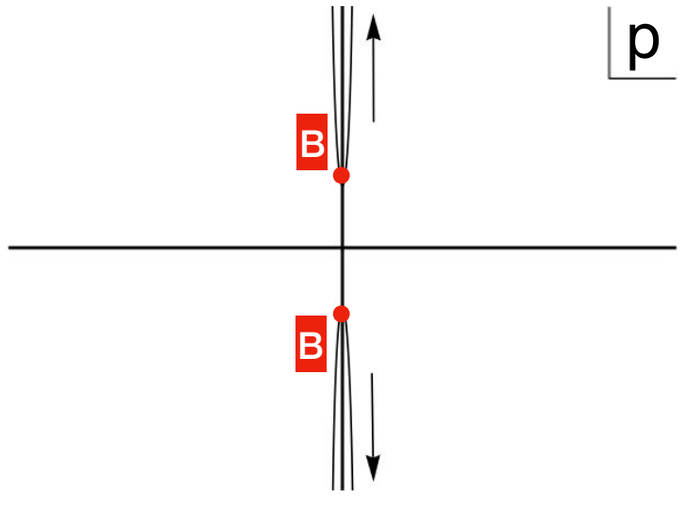
Three-body cut

$m_\pi < m_{D^*} - m_D$



Left-hand cut

$m_\pi > m_{D^*} - m_D$



Additional slides for Tbc

M. Abolnikov, L. Meng, VB, E. Epelbaum, A. Filin, A. Gasparyan arXiv:2602.02176 [hep-ph], accepted for PRD (2026)

EFT for T_{bc} states

- LO coupled-channel effective potentials fulfilling HQSS

HQSS

$A_1^+[0]:\ 0^+:\{BD(^1S_0), B^*D^*(^1S_0)\}$ $\quad T_1^+[0]:\ 1^+:\{B^*D(^3S_1), BD^*(^3S_1), B^*D^*(^3S_1)\}$ $\quad 2^+:\{B^*D^*(^5S_2)\}$

$$V^{(0)}_{\rm cont}[0^+] = \begin{pmatrix} \mathcal{C}_d+\mathcal{C}_f & \sqrt{3}\,\mathcal{C}_f \\ \sqrt{3}\,\mathcal{C}_f & \mathcal{C}_d-\mathcal{C}_f \end{pmatrix} \qquad V^{(0)}_{\rm cont}[1^+] = \begin{pmatrix} \mathcal{C}_d+\mathcal{C}_f & \mathcal{C}_f & \sqrt{2}\mathcal{C}_f \\ \mathcal{C}_f & \mathcal{C}_d+\mathcal{C}_f & -\sqrt{2}\mathcal{C}_f \\ \sqrt{2}\mathcal{C}_f & -\sqrt{2}\mathcal{C}_f & \mathcal{C}_d \end{pmatrix} \qquad V^{(0)}_{\rm cont}[2^+] = \mathcal{C}_d + 2\,\mathcal{C}_f$$

$$V^{(0)}_{\rm OPE}[0^+] = \begin{pmatrix} 0 & V^{B\bar{D}\to B^*\bar{D}^*}_{\rm OPE} \\ V^{B^*\bar{D}^*\to B\bar{D}}_{\rm OPE} & V^{B^*\bar{D}^*\to B^*\bar{D}^*}_{\rm OPE} \end{pmatrix} \qquad V^{(0)}_{\rm OPE}[1^+] = \begin{pmatrix} 0 & V^{B^*\bar{D}\to B\bar{D}^*}_{\rm OPE} & V^{B^*\bar{D}\to B^*\bar{D}^*}_{\rm OPE} \\ V^{B\bar{D}^*\to B^*\bar{D}}_{\rm OPE} & 0 & V^{B^*\bar{D}\to B^*\bar{D}^*}_{\rm OPE} \\ V^{B^*\bar{D}^*\to B^*\bar{D}}_{\rm OPE} & V^{B^*\bar{D}^*\to B\bar{D}^*}_{\rm OPE} & V^{B^*\bar{D}^*\to B^*\bar{D}^*}_{\rm OPE} \end{pmatrix} \qquad V^{(0)}_{\rm OPE}[2^+] = V^{B^*\bar{D}^*\to B^*\bar{D}}_{\rm OPE}$$

⇒ LO contact potentials for different J^{PC} depend of two parameters C_d and C_f

⇒ Lowest channels: EFV receive OPE effects only from off-diag. transitions

No diagonal OPE in contrast to Tcc!

- Extension to higher orders via:

$$\mathcal{C}_d \to \mathcal{C}_d + \mathcal{D}_d(p^2+p'^2) + \cdots$$
$$\mathcal{C}_f \to \mathcal{C}_f + \mathcal{D}_f(p^2+p'^2) + \cdots$$

- Lippmann-Schwinger Eq. in FV:

$$\mathbb{T}^{\alpha\beta}(E) = \mathbb{V}^{\alpha\beta}(E) + \mathbb{V}^{\alpha\gamma}(E)\mathbb{G}^{\gamma}(E)\mathbb{T}^{\gamma\beta}(E)$$

EFT2: Coupled-channel EFT for T_{bc} states

Fit nomenclature:

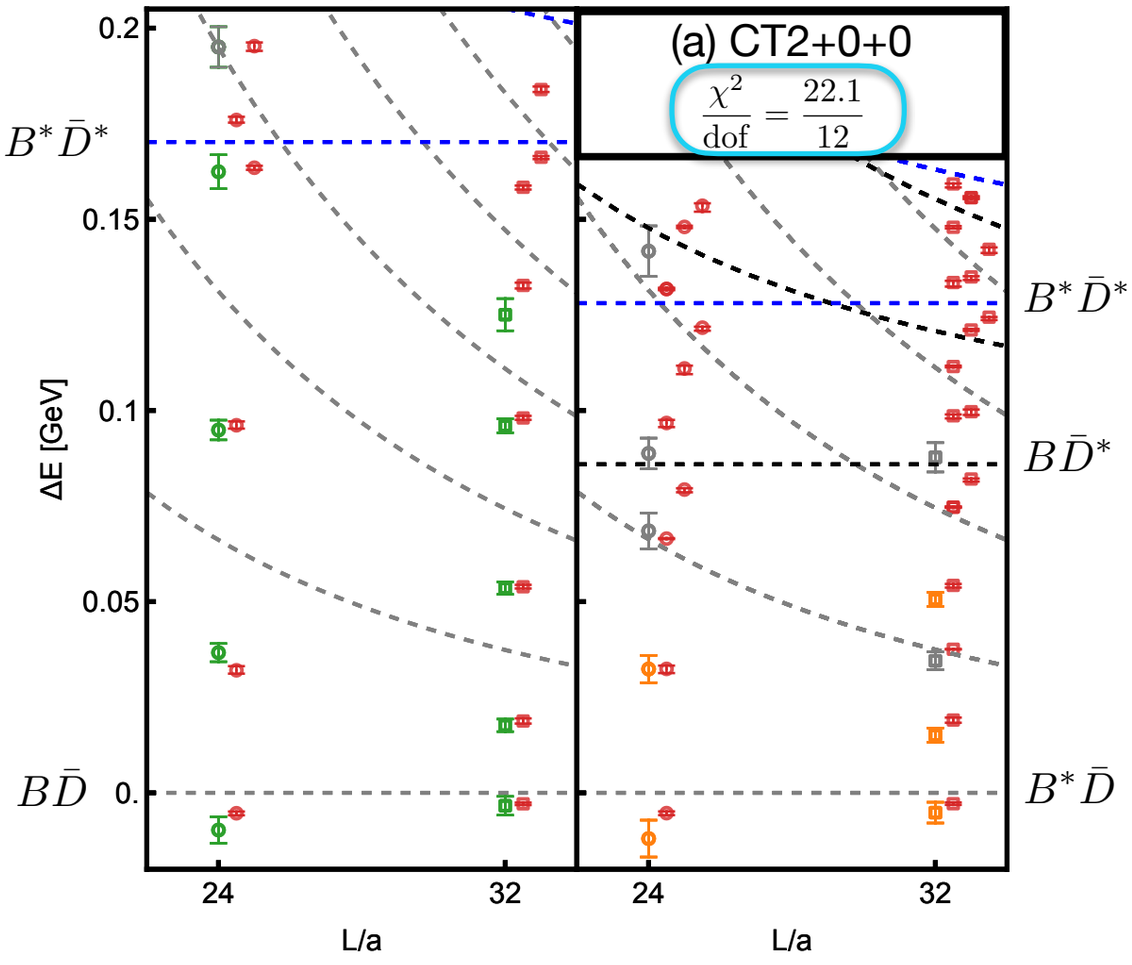
$\#$ of diag CTs $\#$ of $\mathcal{C}_f$ $\#$ of $\mathcal{D}_f(p^2+p'^2)$

Contact: $\mathrm{CT}N_d + N_{C_f} + N_{D_f}$

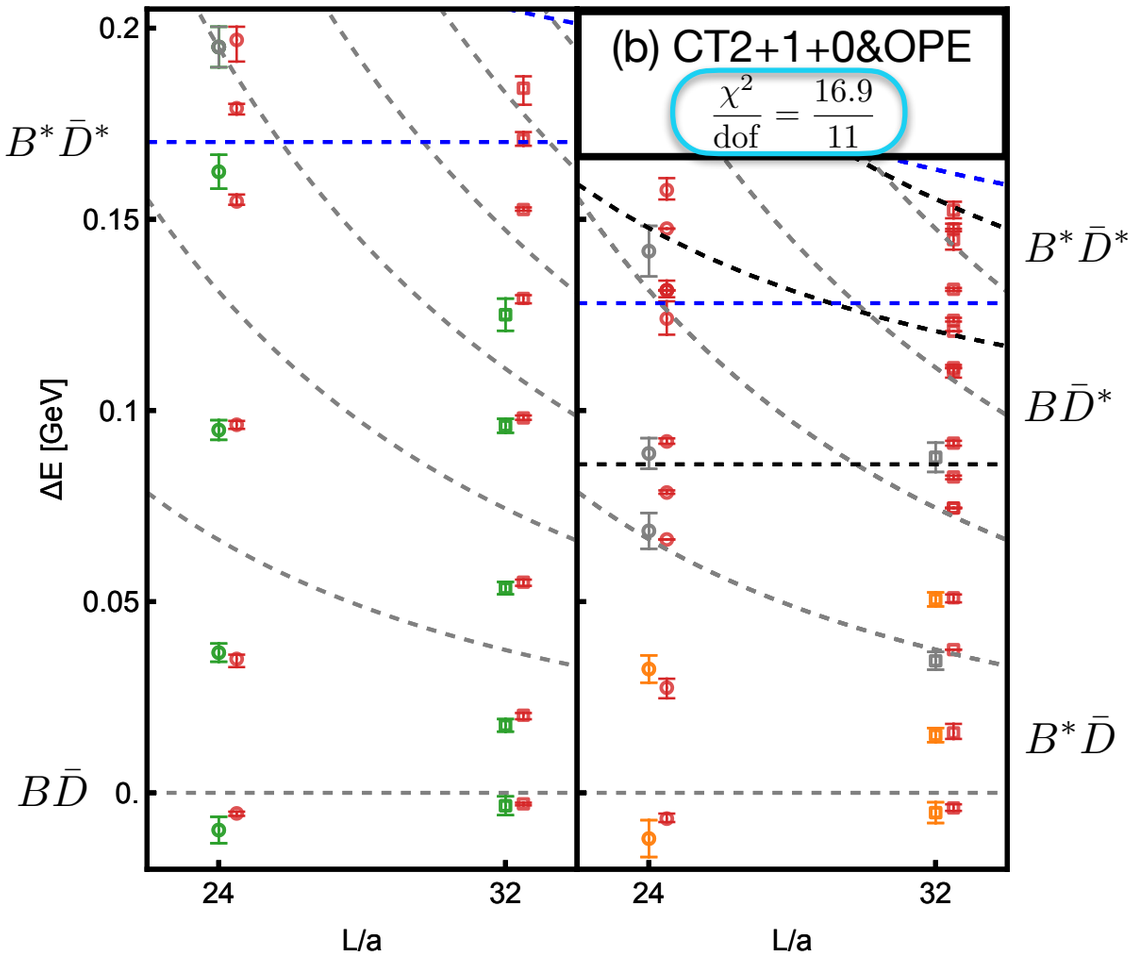
Contact + OPE: $\mathrm{CT}N_d + N_{C_f} + N_{D_f}$&OPE

Fits to all data

Single channel 2 param



Coupled-channel 3 param



⇒ Some improvement in the fit quality

But: — No effect on the lowest levels

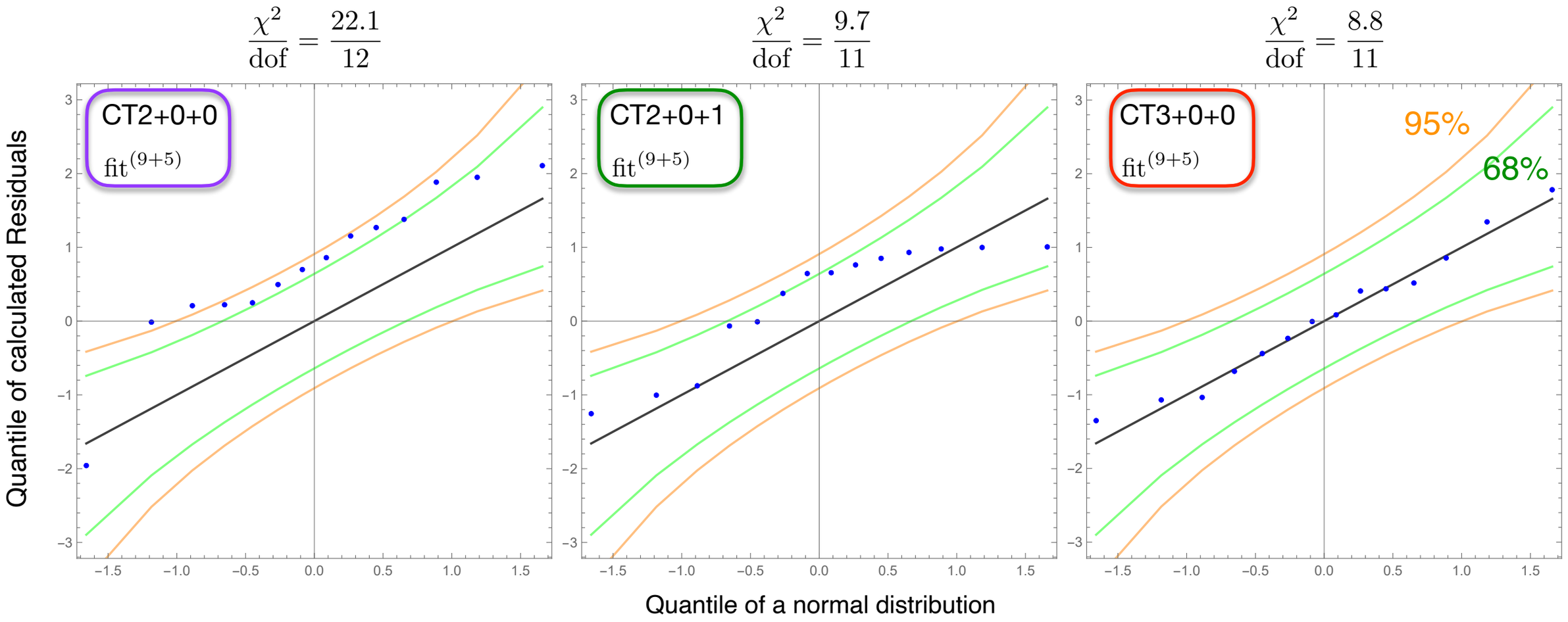
— Quantile-Quantile plots show deviations from the normal distributions

— The effect of OPE is weak

Quantile-Quantile Plots: EFT2

- Consistency check: theory vs normal distribution

$$\mathrm{Res}_i = \frac{E^{\mathrm{EFT}}(i) - E^{\mathrm{LQCD}}(i)}{\Delta E^{\mathrm{LQCD}}(i)}$$



x = y line:	strong deviations	strong deviations	closely follow
68% band:	many data points fall above	some data points beyond	all data points within
95% band:	some beyond	all within	all within
	⇒ Not normal	⇒ Sizeable deviations from normal	⇒ Normal

EFT2: Coupled-channel EFT for T_{bc} states

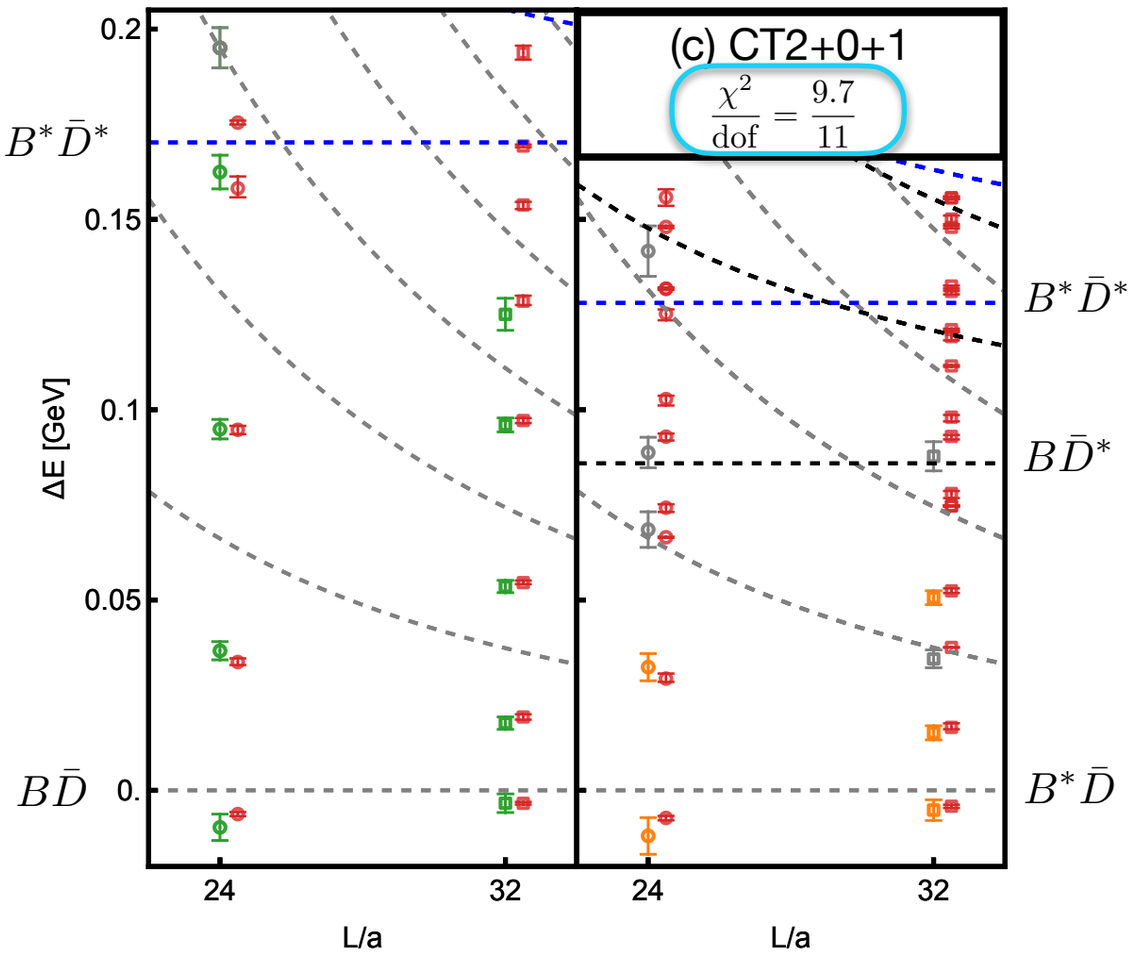
Fit nomenclature:

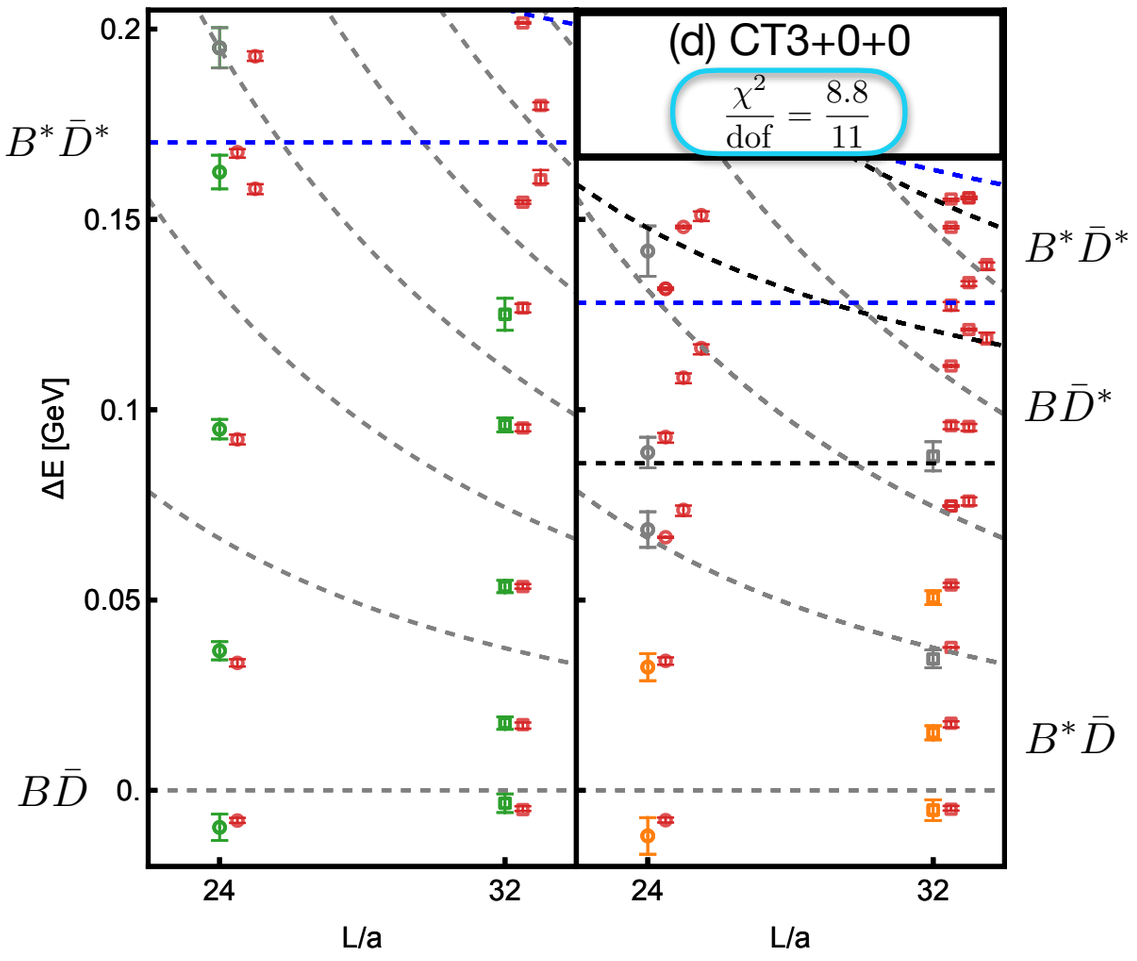
$\#$ of diag CTs $\#$ of $\mathcal{C}_f$ $\#$ of $\mathcal{D}_f(p^2+p'^2)$

Contact: $\mathrm{CT}N_d + N_{C_f} + N_{D_f}$

Contact + OPE: $\mathrm{CT}N_d + N_{C_f} + N_{D_f}$ &OPE

Fits to all data





χ^2 :	a little worse	comparable	a little better
Description low-energy levels	worse		better
QQ plots:	Deviations from normal distr.		Consistent with normal distr.

And what about pions?

- Comparing CT3+0+0 vs CT3+1+0&OPE

$$\frac{\chi^2}{\text{dof}} = \frac{8.8}{11} \qquad \frac{\chi^2}{\text{dof}} = \frac{8.5}{10}$$

		fit CT3+0+0		fit CT3+1+0&OPE	
Threshold	J^P	Pole [MeV]	RS	Pole [MeV]	RS
$B\bar{D}$	0^+	-0.8	$(+)$	-1.0	$(++)$
$B^*\bar{D}^*$	0^+	-7.6	$(+)$	$-6.7-0.4i$	$(-+)$
$B^*\bar{D}$	1^+	-0.7	$(+)$	-0.9	$(+++)$
$B\bar{D}^*$	1^+	-8.0	$(+)$	$-8.3-0.3i$	$(-++)$
$B^*\bar{D}^*$	1^+	-7.6	$(+)$	$-7.1-0.7i$	$(--+)$
$B^*\bar{D}^*$	2^+	-7.6	$(+)$	-8.4	$(+)$

- OPE: breaks degeneracy in B*D* poles

  poles acquire Im parts ⇒ decay to lower channels

- But current data are weakly sensitive to OPE

⇒ Key probe: lattice data in the higher channels!

Cutoff dependence

EFT1:

CT2+0+0:

$$V_{\rm cont} = \mathcal{C}_d + \mathcal{D}_d(p^2 + p'^2)$$

⇒ Negligible

EFT2:

CT2+0+0:

$$V_{\rm cont} = \mathcal{C}_d + \mathcal{D}_d(p^2 + p'^2)$$

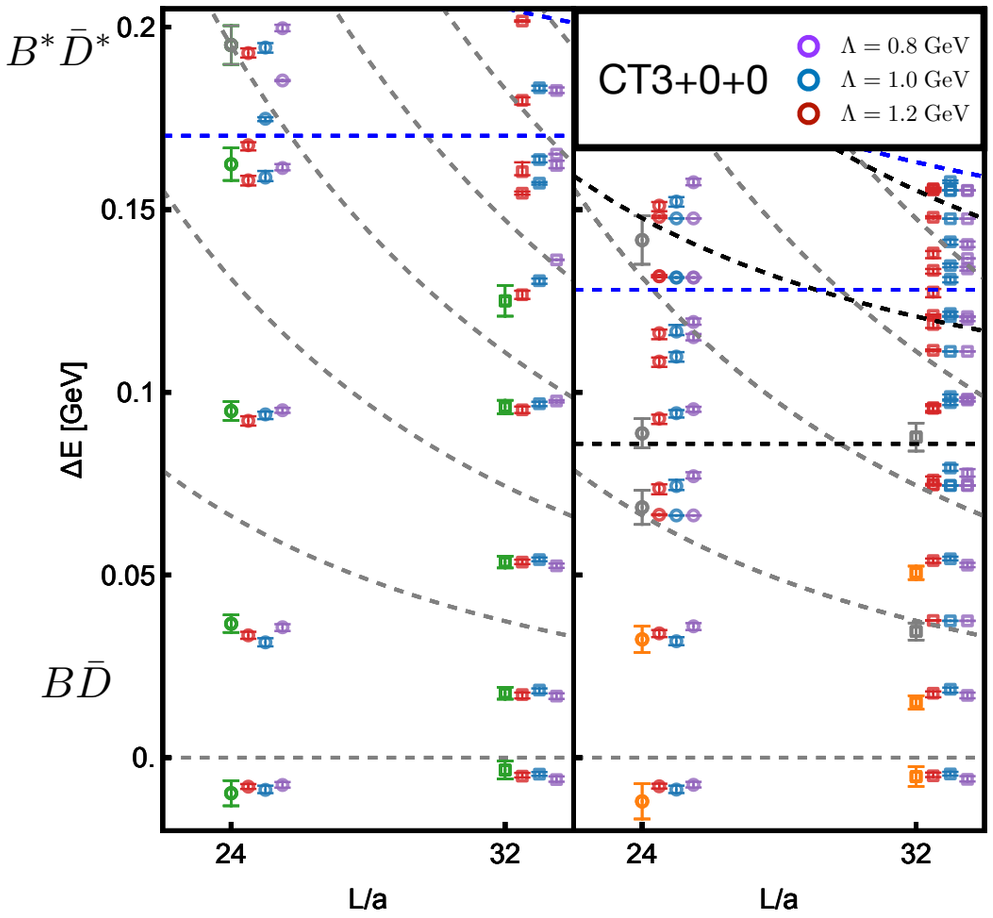
⇒ Pronounced due to unphysical poles below threshold

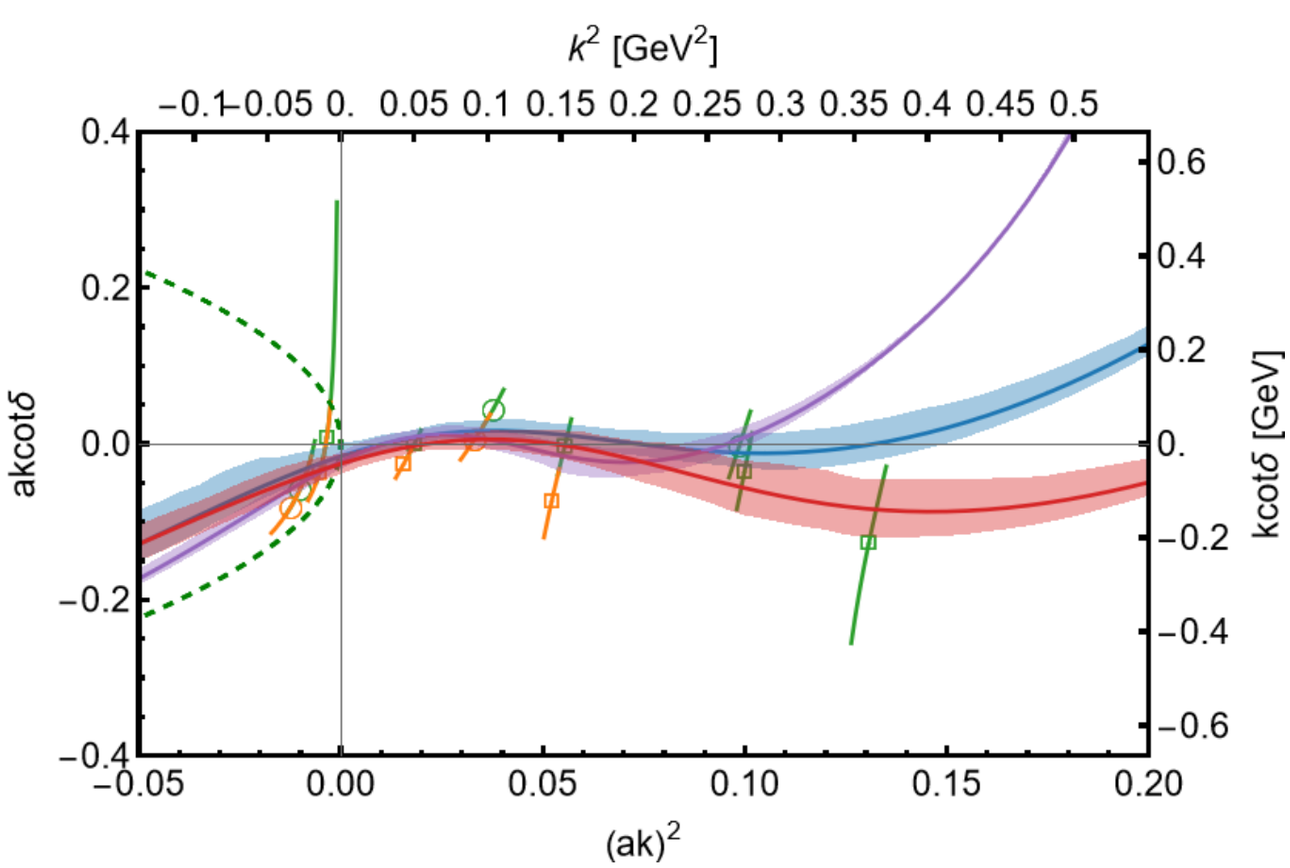
CT3+0+0:

$$V_{\rm cont} = \mathcal{C}_d + \mathcal{D}_d(p^2 + p'^2) + \mathcal{E}_d(p^4 + p'^4)$$

⇒ Largely cutoff independent up to k= 450 MeV

⇒ At larger k, onset of a pole in kcotδ

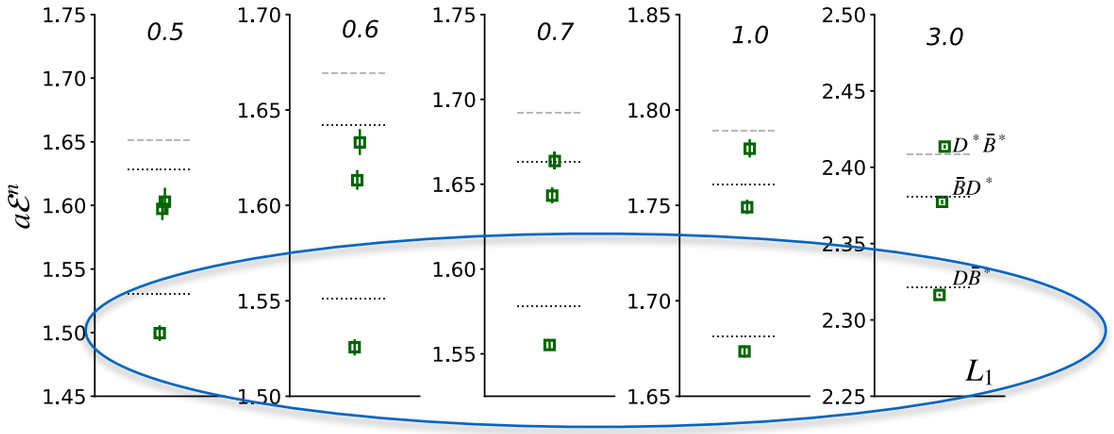


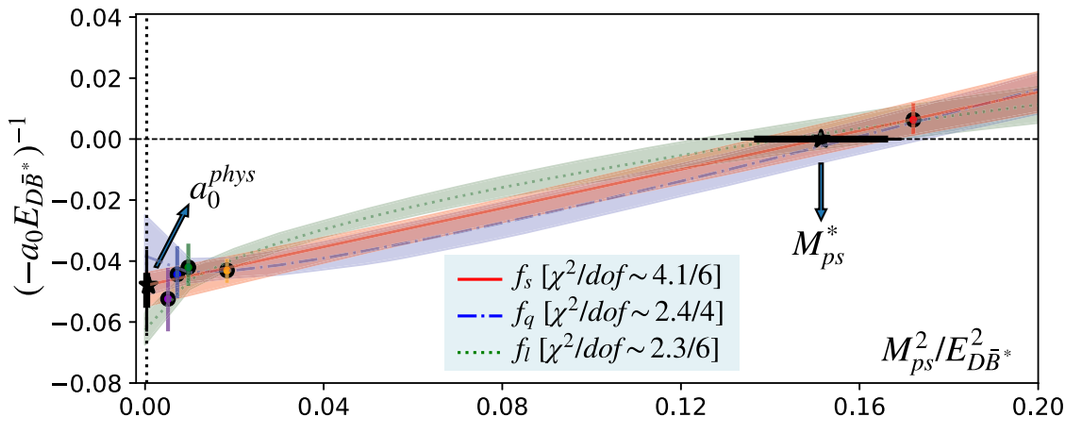


T_{bc} from lattice QCD in finite volume $\bar{b}\bar{c}qq$

Radhakrishnan, Padmanath, Mathur PRL 132, 201902 (2024) , PRD 110, 034506 (2024)

$I=0, J^P=1^+$





- Local four-quark + two-meson scattering operators
- Ground state levels for different pseudoscalar masses from 0.5 to 3.0 GeV
- Lüscher single-channel analysis of ground state levels for BD (J=0) and B*D (J=1) ⇒ scattering lengths
- Polynomial extrapolation to the continuum limit and the phys. light quark mass

— Two not so shallow bound T_{bc} states

$$\delta m_{T_{bc}} = -43\,\binom{+6}{-7}\,\binom{+14}{-24}\ \text{MeV} \qquad I=0, J^P=1^+$$

$$\delta m_{T_{bc}} = -39\,\binom{+4}{-6}\,\binom{+8}{-18}\ \text{MeV} \qquad I=0, J^P=0^+$$

- No long-range interactions with lhc's, no coupled-channel effects, no consequences from HQSS

T_{bc} from lattice QCD in finite volume $\bar{b}\bar{c}qq$

Hoffmann, Müller and Wagner, PoSLAT- TICE2024, 091 (2025), 2501.16188

- Born–Oppenheimer approximation using antistatic-antistatic potentials computed with lattice QCD from P. Bicudo et al, PRD 93, 034501 (2016), 1510.03441.

- Three values of the pion mass between 340 and 650 MeV

- Extrapolation to the physical light quark mass

- Two deeply virtual isoscalar T_{bc} states with $J^P = 1^+$ and $J^P = 0^+$ both ~ 100 MeV below thresh.

- Potential reason for the difference: underestimated attraction of some potentials

  $\Rightarrow$ calculations using significantly improved up-to-date lattice QCD setup are initiated

Additional slides for Tcc

Meng, VB, Filin, Epelbaum and Gasparyan *PRD letter* 109, L071506 (2024)

Meng, Ortiz-Pacheco, VB, Epelbaum , Padmanath and Prelovsek e-Print: 2411.06266 [hep-lat] (2024)

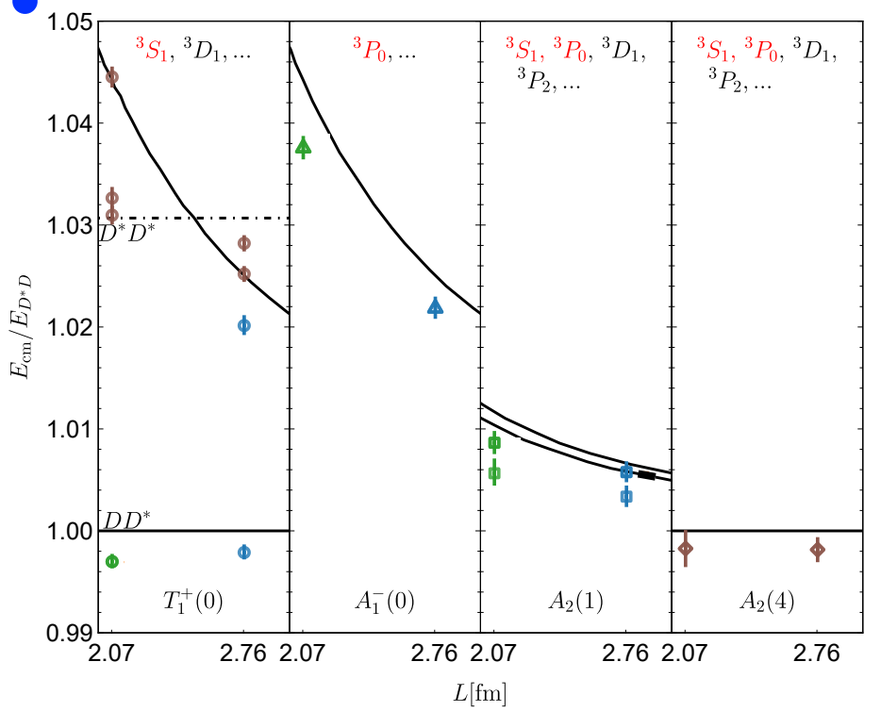
M. Abolnikov, VB, E. Epelbaum, A. Filin, C. Hanhart and L. Meng PLB 860 139188 (2025)

App I: I=0 DD* scattering in FV

Meng, VB, Filin, Epelbaum and Gasparyan *PRD letter* 109, L071506 (2024)

Padmanath and Prelovsek, PRL 129,032002 (2022)

- Lattice $m_\pi = 280\,\mathrm{MeV}$



EFV are below the D*D* thr ⇒ single channel DD* EFT to NLO

$$V = V^{(0)}_{\rm OPE} + V^{(0)}_{\rm cont} + V^{(2)}_{\rm cont} + \ldots$$

$$V^{(0)+(2)}_{\rm cont}[^3S_1] = \left(C^{(0)}_{^3S_1} + C^{(2)}_{^3S_1}(p^2 + p'^2)\right)(\vec{\epsilon}\cdot\vec{\epsilon}'^*)$$

$$V^{(2)}_{\rm cont}[^3P_0] = C^{(2)}_{^3P_0}\,(\vec{p}'\cdot\vec{\epsilon}'^*)(\vec{p}\cdot\vec{\epsilon})$$

Take care of m_π dependence of $m_{D(*)}$, f_π and $g_{D^*D\pi}$

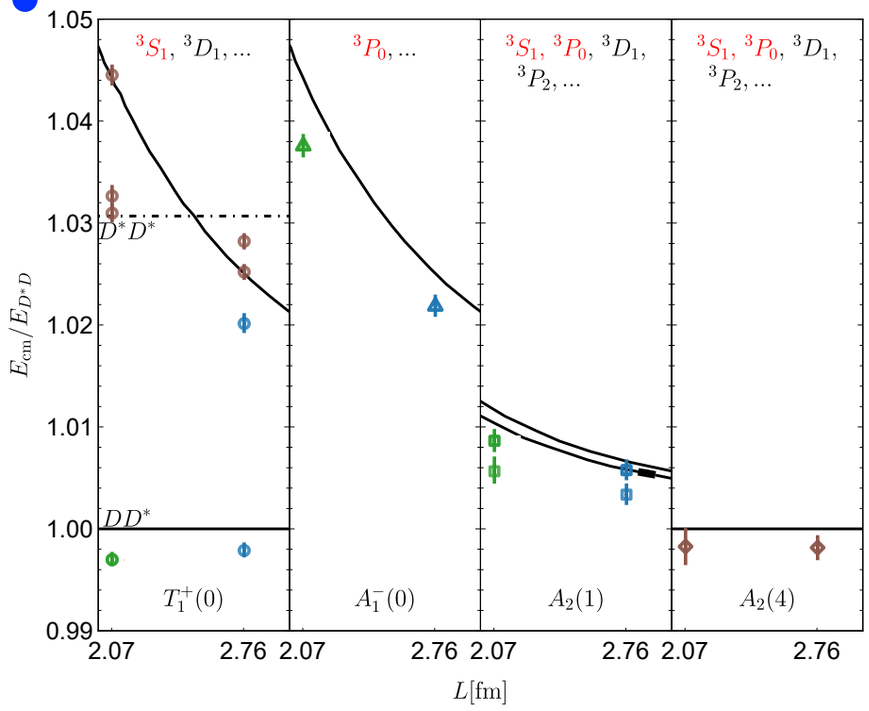
Cleven et al. EPJA 47 (2011) 19;
VB et al. PLB 726 (2013) 537

App I: I=0 DD* scattering in FV

Meng, VB, Filin, Epelbaum and Gasparyan *PRD letter* 109, L071506 (2024)

Padmanath and Prelovsek, PRL 129,032002 (2022)

- Lattice $m_\pi = 280\,\mathrm{MeV}$



EFV are below the D*D* thr ⇒ single channel DD* EFT to NLO

$$V = V^{(0)}_{\rm OPE} + V^{(0)}_{\rm cont} + V^{(2)}_{\rm cont} + \ldots$$

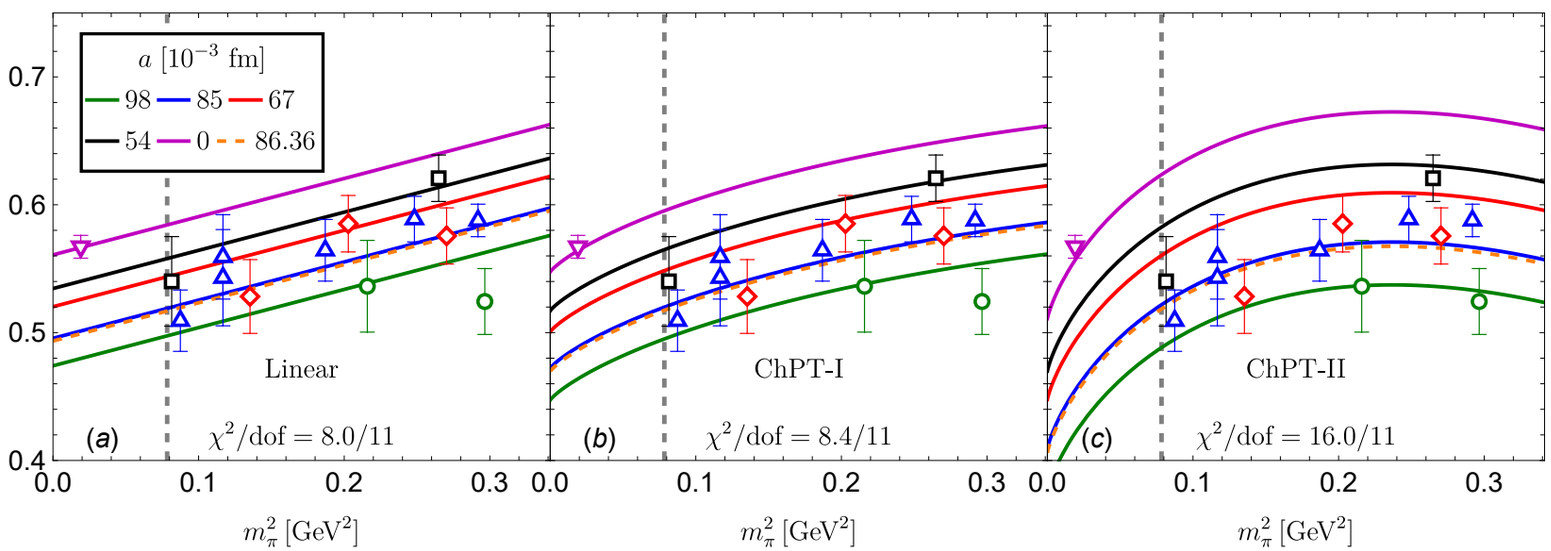
$$V^{(0)+(2)}_{\rm cont}[^3S_1] = \left(C^{(0)}_{^3S_1} + C^{(2)}_{^3S_1}(p^2 + p'^2)\right)(\vec{\epsilon}\cdot\vec{\epsilon}'^*)$$

$$V^{(2)}_{\rm cont}[^3P_0] = C^{(2)}_{^3P_0}\,(\vec{p}'\cdot\vec{\epsilon}'^*)(\vec{p}\cdot\vec{\epsilon})$$

Take care of m_π dependence of $m_{D(*)}$, f_π Cleven et al. EPJA 47 (2011) 19; VB et al. PLB 726 (2013) 537

and $g_{D^*D\pi}$

$g_{D^*D\pi}$: two parameter fits to lattice (Becirevic and Sanfilippo PLB 721 (2013) 94) + physical value: $g \equiv g(a, m_\pi)$



$g \equiv g(0.08636, 0.280)$

	g_0	α [GeV^{-2}]	β [fm^{-2}]	g
Linear	0.561(9)	0.53(13)	−16.1(44)	0.517(15)
ChPT-I	0.541(8)	0.10(14)	−20.5(45)	0.518(15)
ChPT-II	0.511(8)	−0.59(15)	−27.6(48)	0.519(15)

Truncation uncertainty of chiral expansion

M. Abolnikov, VB, E. Epelbaum, A. Filin, C. Hanhart and L. Meng PLB 860 139188 (2025)

Add higher-order interactions + naturalness

$$V = V^{(0)}_{\rm OPE} + V^{(0)}_{\rm cont} + V^{(2)}_{\rm cont} + V^{(4)}_{\rm cont}$$

$$V^{(0)+(2)}_{\rm cont}[^3S_1] = C^{(0)}_{^3S_1} + C^{(2)}_{^3S_1}(p^2 + p'^2) + D^{(2)}_{^3S_1}(\xi^2 - 1)$$

Fits

$$C_2 = \frac{\alpha_2}{F_\pi^2}\frac{1}{\Lambda_\chi^2}; \quad \alpha_2 = 0.2$$

$$D_2 = \frac{\tilde\alpha_2}{F_\pi^2}\left(\frac{m_\pi^{\rm ph}}{\Lambda_\chi}\right)^2; \quad \tilde\alpha_2 = 0.4$$

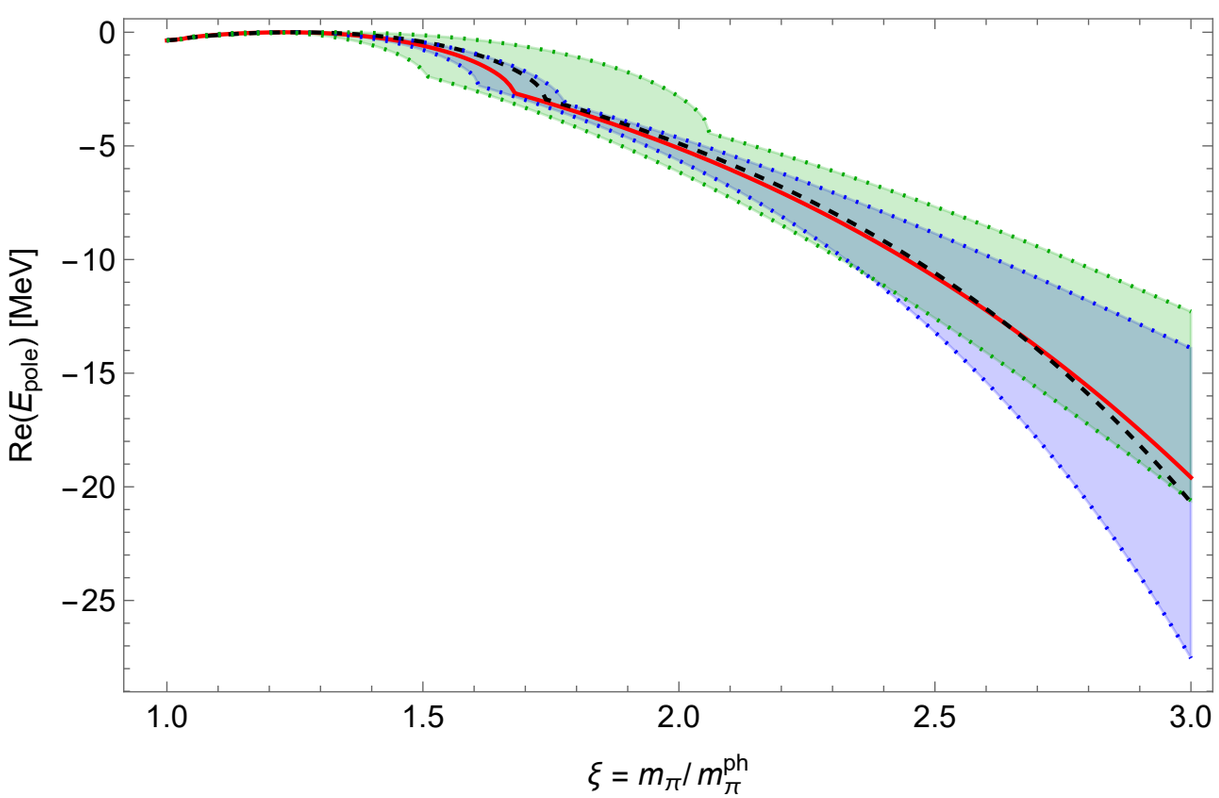
Naturalness

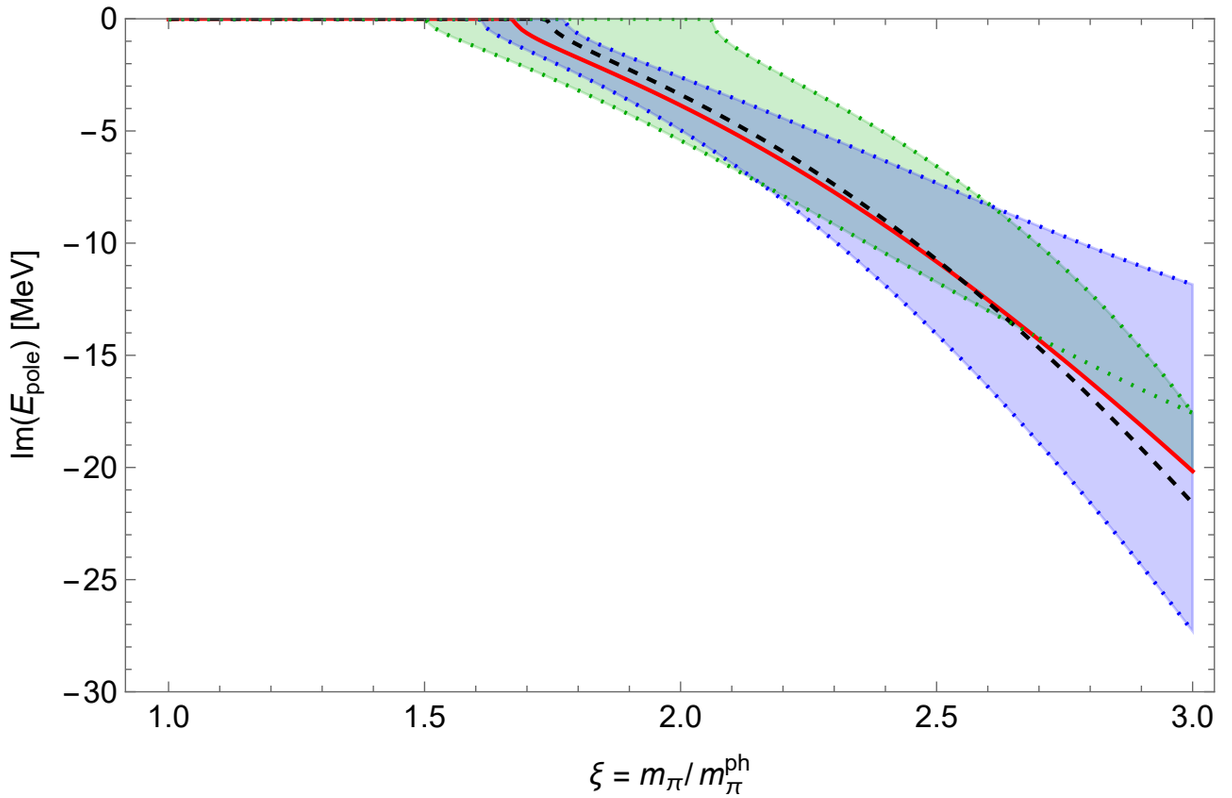
$$V^{(4)}_{\rm cont} = D_4(\xi^2 - 1)(p^2 + p'^2) + \tilde D_4(\xi^4 - 1)$$

$$D_4 = \frac{\alpha_4}{F_\pi^2}\left(\frac{m_\pi^{\rm ph}}{\Lambda_\chi^2}\right)^2; \quad \alpha_4 \in [-1, 1]$$

$$\tilde D_4 = \frac{\tilde\alpha_4}{F_\pi^2}\left(\frac{m_\pi^{\rm ph}}{\Lambda_\chi}\right)^4; \quad \tilde\alpha_4 \in [-1, 1]$$

⇒ Comparable with statistical uncertainty



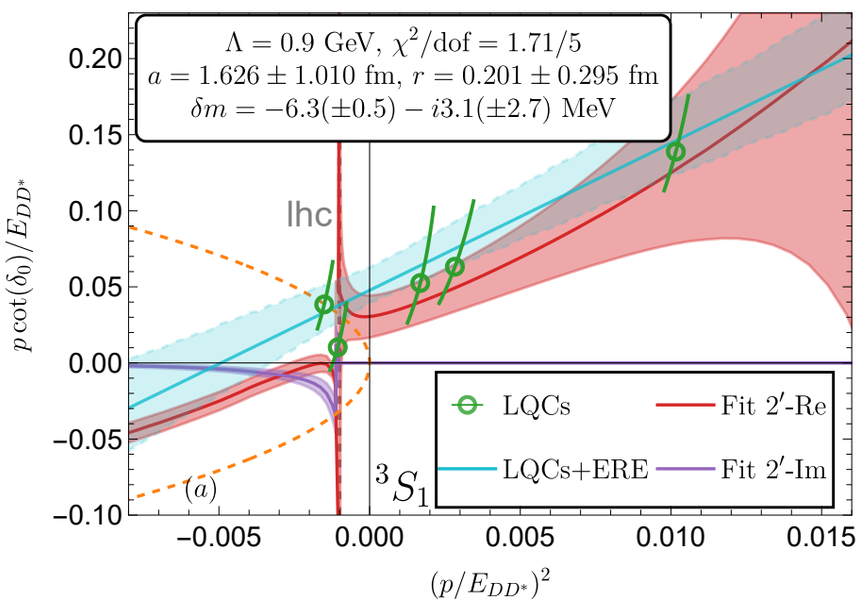


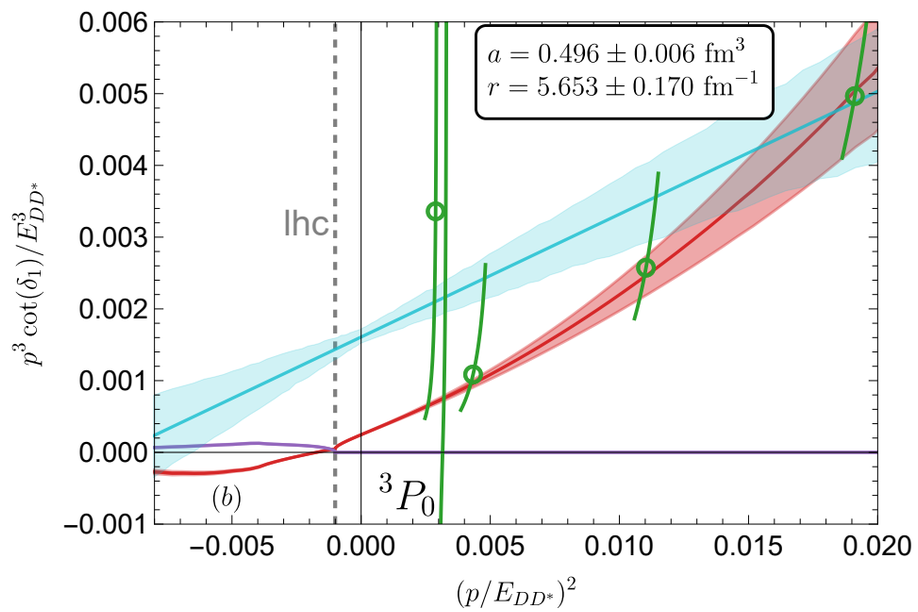
Testing chiral truncation uncertainty at $m_\pi = 280$ MeV

Meng, VB, Filin, Epelbaum and Gasparyan *PRD letter* 109, L071506 (2024)

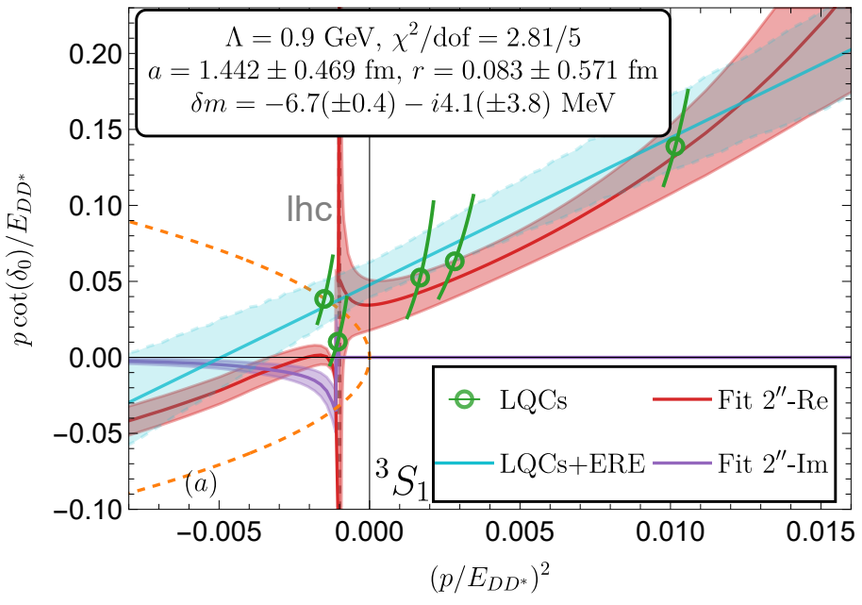
- Additional contact terms

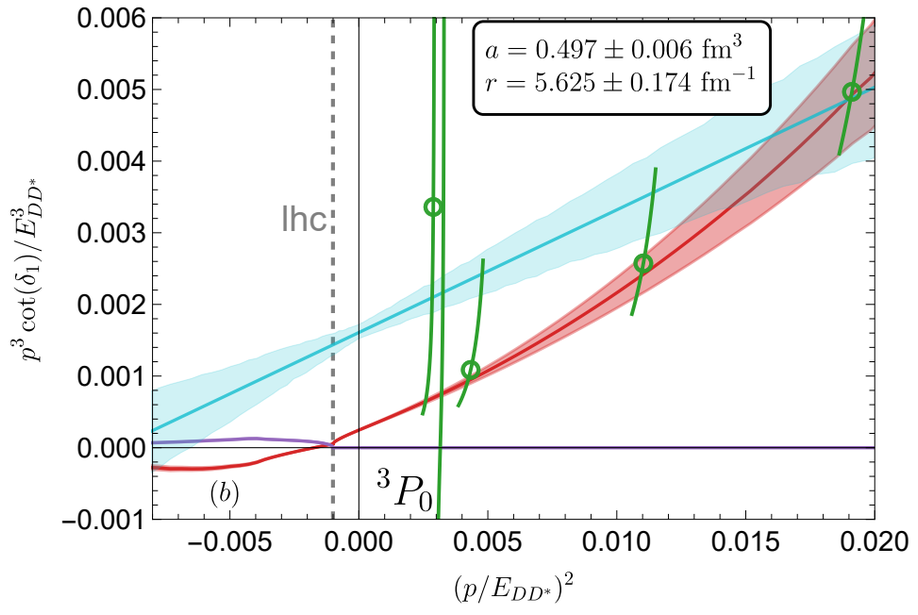
$$V^{(2)}_{\rm cont}[^3S_1 - {}^3D_1] = C^{(2)}_{SD}\, p'^2$$





$$V^{(2)}_{\rm cont}[^3P_2] = C^{(2)}_{^3P_2}$$





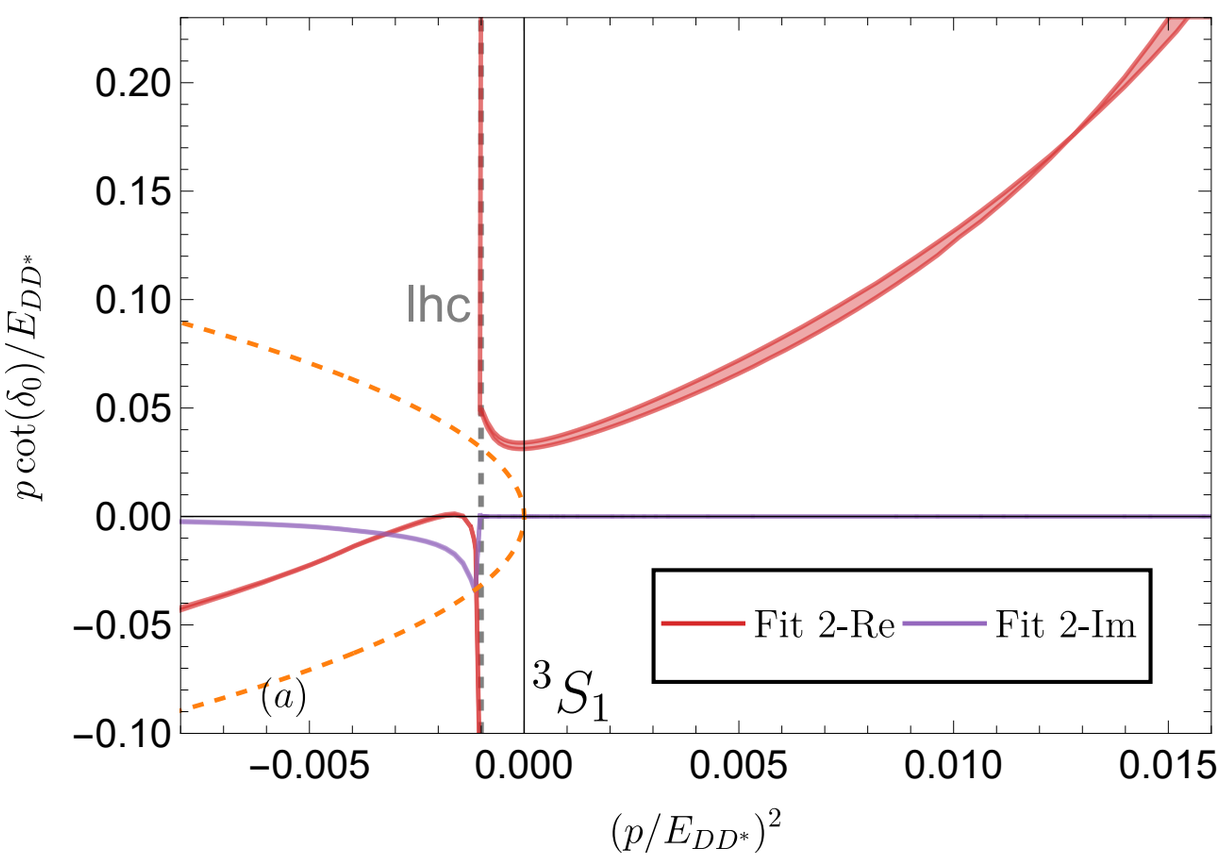
$\Rightarrow$ Some effect of the S-D term on phase shifts at larger momenta

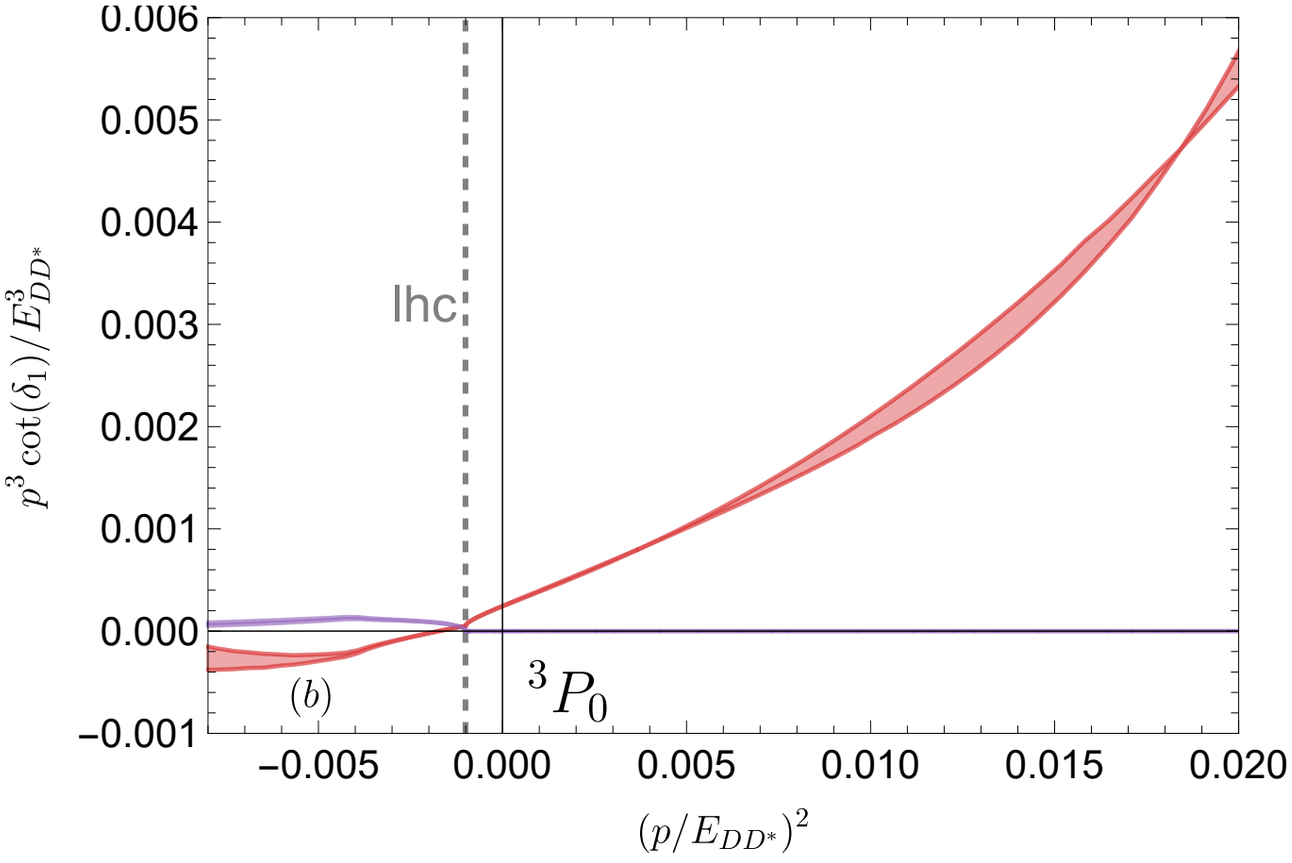
$\Rightarrow$ The impact near the threshold and on the pole is minor

I=0 DD* scattering: Residual cutoff dependence

Meng, VB, Filin, Epelbaum and Gasparyan *PRD letter* 109, L071506 (2024)

- Cutoff variation from 0.7 to 1.2 GeV





$\Rightarrow$ very small

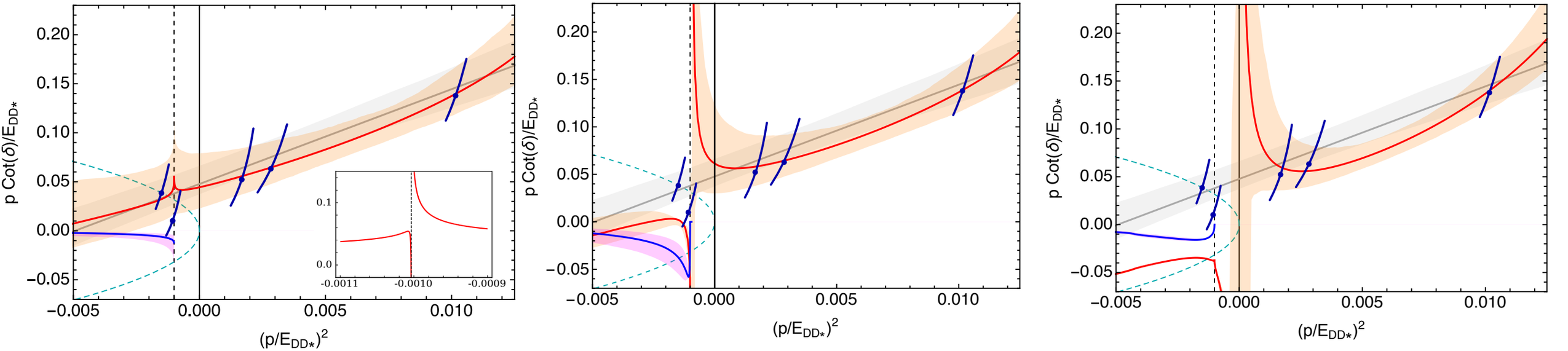
Dependence on the pion coupling

M. Du, A. Filin, VB, X. Dong, E. Epelbaum, F.-K. Guo, C. Hanhart, A. Nefediev, J. Nieves and Q. Wang *PRL* 131, 131903 (2023)

Repulsive OPE:

- Importance of lhc for the given m_π is controlled by its position and strength (residue)

$\frac{1}{10} V^{\rm OPE}_{{\rm DD}^*\to{\rm DD}^*}(m_\pi = 280{\rm MeV})$ $V^{\rm OPE}_{{\rm DD}^*\to{\rm DD}^*}(m_\pi = 280{\rm MeV})$ $5\ V^{\rm OPE}_{{\rm DD}^*\to{\rm DD}^*}(m_\pi = 280{\rm MeV})$

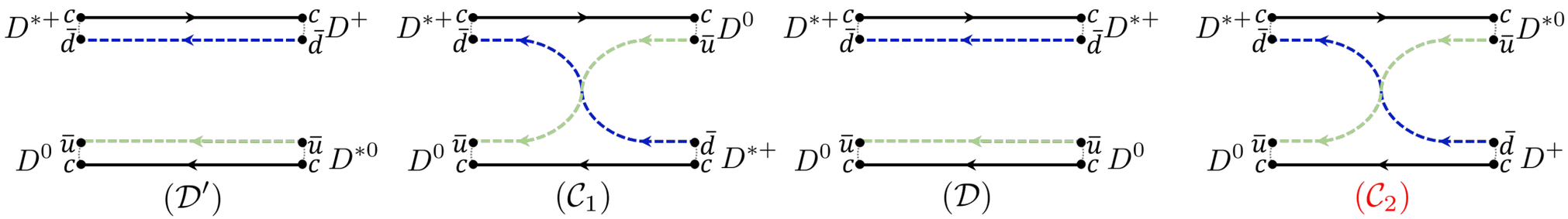


- The smaller the coupling, the closer the fit is to the ERE

  → see I=1 DD* scattering

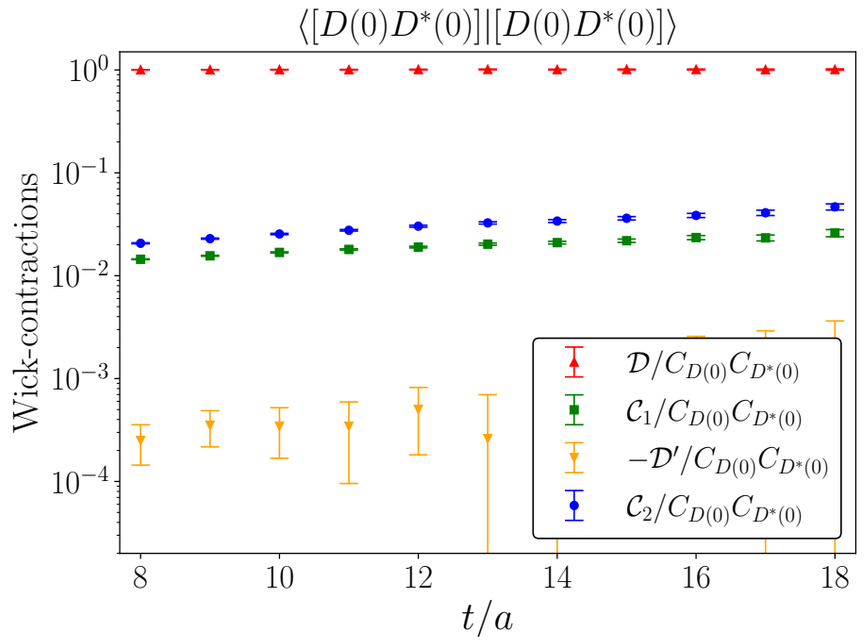
Isoscalar vs Isovector: what makes the difference?

Meng, Ortiz-Pacheco, VB, Epelbaum, Padmanath and Prelovsek PRD 111, 034509 (2025)



$$\langle (DD^*)_I | (DD^*)_I \rangle = \mathcal{D} - \mathcal{C}_1 + (-1)^{I+1}(\mathcal{D}' - \mathcal{C}_2)$$

$$(DD^*)_I = \frac{1}{\sqrt{2}}[D^0 D^{*+} + (-1)^{I+1} D^+ D^{*0}]$$



in line with CLQCD: Chen et al. PLB 833 2022

- D′ and C_2 contribute to the difference but D′ << C_2
- C_2: no pseudoscalars because of parity

charge exchange ⇒ vector isovector contribution due to two-pion or rho-exchange

$$\langle (DD^*)_I | \boldsymbol{\tau}^{(1)} \cdot \boldsymbol{\tau}^{(2)} | (D^*D)_I \rangle_{\mathcal{C}_2} = \begin{cases} -2\ ;\ I=0 & \text{attraction} \\ 2\ ;\ I=1. & \text{repulsion} \end{cases}$$

- Consistent with that two-pion exchange for DD* is attractive for I=0 and repulsive for I=1

Chacko, VB, Hanhart and Krug, *Phys.Rev.D* 111, 3 (2025)